CHEMISTRY
A EUROPEAN JOURNAL

FULL PAPER

DOI: 10.1002/chem.200((will be filled in by the editorial staff))

Synthesis and Reactivity of Mononuclear Iron Models of [Fe]-Hydrogenase that Contain an Acylmethylpyridinol Ligand

Bowen Hu,[a] Dafa Chen*[a] and Xile Hu[b]

Dedication ((optional))

Abstract: [Fe]-hydrogenase has a mono-iron containing active site that features an acylmethylpyridinol ligand. This unique ligand environment has yet to be reproduced in synthetic models. Herein, we report the synthesis and reactivity of a new class of small molecule mimics of [Fe]-hydrogenase in which a mono-iron center is ligated by an acylmethylpyridinol ligand. Key to the preparation of these model compounds is the successful C-O cleavage of an alkyl ether moiety to form the desired pyridinol ligand. Reaction of solvated complex [(2-CH_2CO-6-HOC_5H_3N)$Fe(CO)_2(CH_3CN)_2]^+(BF_4)^-$ (**6**) with thiols or thiophenols in the presence of NEt_3 yielded 5-coordinate iron thiolate complexes (**7**-**11**). Further derivation produced complexes [(2-CH_2CO-6-HOC_5H_3N)$Fe(CO)_2(SCH_2CH_2OH)$] (**12**) and [(2-CH_2CO-6-HOC_5H_3N)$Fe(CO)_2(CH_3COO)$] (**13**), which could be regarded as models of (methenyl-H_4MPT^+).[1,2] 2-mercaptoethanol and acetic acid extracted FeGP cofactors of [Fe]-hydrogenase, respectively. When complexes **7**-**12** were treated with $HBF_4{\cdot}Et_2O$, **6** was regenerated, *via* a protonation of the thiolate ligands. The reactivity of several models with CO, isocyanide, cyanide and H_2 was also investigated.

Keywords: Enzyme models • hydrogenases • iron • carbonyl complexes • thiolate

Introduction

Hydrogenases are enzymes that catalyze the production or consumption of H_2. Based on the metal atoms in the active site, hydrogenases are classified in three types, namely [FeFe]-, [NiFe]-, and [Fe]-hydrogenases.[1-5] Unlike the other two types of hydrogenases, [Fe]-hydrogenase, which is also called as H_2-forming methylene-tetrahydromethanopterin dehydrogenase (Hmd), does not contain a redox-active site and a [Fe_4S_4] cluster, and can only activate H_2 in the presence of methenyltetrahydromethanopterin (methenyl-H_4MPT^+).[1,2]

In the active site of [Fe]-hydrogenase, a Fe(II) center is coordinated with two *cis*-CO, a cysteine sulfur atom (Cys 176), and a bidentate acylmethylpyridinol ligand. The sixth position, which is regarded as the H_2-binding position, is probably occupied by a labile water molecule (Figure 1).[6-8]

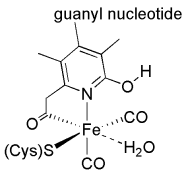

Figure 1. The active site of [Fe]-hydrogenase.

The iron guanylylpyridinol (FeGP) cofactor of [Fe]-hydrogenase can be extracted by denaturation of the enzyme in the presence of 2-mercaptoethanol or acetic acid.[9-13] If the FeGP cofactor is mixed with the apoenzyme, an active [Fe]-hydrogenase would be reconstituted. The structures of the protein-free cofactors were proposed accordingly as in Figure 2, and they were confirmed by mass spectrometry.[12,13]

[a] Dr. B. Hu, Prof. Dr. D. Chen
School of Chemical Engineering & Technology
Harbin Institute of Technology
Harbin 150001, P.R. China
E-mail: dafachen@hit.edu.cn

[b] Prof. Dr. X. Hu
Laboratory of Inorganic Synthesis and Catalysis
Institute of Chemical Sciences and Engineering
Ecole Polytechnique Fédérale de Lausanne (EPFL)
ISIC-LSCI, BCH 3305, Lausanne 1015, Switzerland
Fax: (+) 49 21 693 9305
E-mail: xile.hu@epfl.ch

Supporting information for this article is available on the WWW under http://www.chemeurj.org/ or from the author.

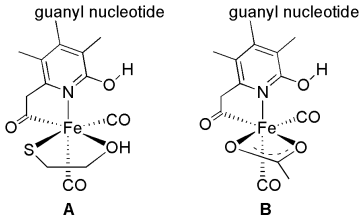

Figure 2. (A) The proposed structure of the FeGP cofactor extracted with 2-mercaptoethanol; (B) The proposed structure of the FeGP cofactor extracted with acetic acid.

Since the elucidation of the structure of [Fe]-hydrogenase, a number of model complexes have been reported.[14-35] Recently we synthesized some 5-coordinate mononuclear iron complexes with a 2-acylmethyl-6-methoxy-pyridyl ligand, which was a mimic to the acylmethylpyridinol ligand in the enzyme. However, the hydroxyl group of the pyridinol ligand in the enzyme might carry a crucial function for H_2 activation.[36,37] The faithful reproduction of such secondary ligand environment in a model complex, therefore, is a desirable goal in biomimetic chemistry. However, only a dinuclear iron complex with an acylmethylpyridinol ligand has been reported; such a complex does not mimic the mononuclear nature of [Fe]-hydrogenase and is not suitable for further reactivity study.[35] Herein, we report the synthesis and reactivity of the first mononuclear model complexes of [Fe]-hydrogenase that contain the previously elusive acylmethylpyridinol ligand.

Results and Discussion

Iron complexes with 2-acylmethyl-6-*tert*-butoxy-pyridyl ligand

To install a pyridinol ligand, we first decided to incorporate a pyridyl alkoxyl group whose alkyl ether moiety might be cleaved at a later stage. To this end, [(2-CH_2CO-6-*t*-$BuOC_5H_3N$)$Fe(CO)_3I$] (**1**) was prepared by dropwise addition of lithiated 2-*tert*-butoxy-6-methylpyridine to $Fe(CO)_5$, followed by treatment of I_2 (Scheme 1). The ^1H NMR spectrum of **1** in $CDCl_3$ exhibits three signals at 7.73, 7.11 and 6.99 ppm for the pyridyl rings, two doublet at 5.42 and 4.29 ppm for the diastereotopic methylene hydrogens, and one singlet at 1.70 ppm for the *t*-butoxy group.[38] The results indicate a single isomer in the solution. The IR spectrum of **1** shows three ν(CO) absorptions in CH_2Cl_2; In the solid state, **1** displays five absorptions,[38] which might be caused by interactions between molecules in the solid lattice. Similar phenomenon has been found in complex $Fe(S_2C_2H_4)(CO)_2(PMe_3)_2$.[39]

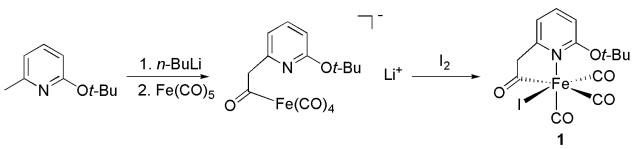

Scheme 1. Synthesis of complex **1**.

Reaction of **1** with $NaS(2,6\text{-}Me_2C_6H_3)$ gave a 5-coordinate complex [2-CH_2CO-6-*t*-$BuOC_5H_3N$)$Fe(CO)_2${S-(2,6-Me_2-C_6H_3)}] (**2**) (Scheme 2), which was characterized by X-ray crystallography (Figure 3). The structure of **2** is similar to that of complex [2-CH_2CO-6-$MeOC_5H_3N$)$Fe(CO)_2${S-(2,6-Me_2-C_6H_3)}].[28] The C(21)-Fe(1)-S(1) angle is 163.5(4)°, and the C(20)-Fe(1)-N(1) angle is 175.5(5)°. Thus, the coordination geometry of the Fe ion is best described as distorted square pyramidal. The bidentate acylmethylpyridyl ligand coordinates with Fe *via* the pyridyl nitrogen and acyl carbon donors. The two CO and the acyl ligands are all mutually *cis*. The sulfur ligand is *cis* to the acyl and pyridyl ligands, and the position *trans* to the acyl ligand is unoccupied. The IR spectrum of **2** shows two equally intense ν(CO) absorptions at 2013 and 1948 cm^{-1} in the solid state, consistent with the existence of two *cis*-CO (Table 1).

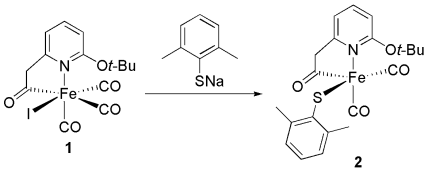

Scheme 2. Synthesis of complex **2**.

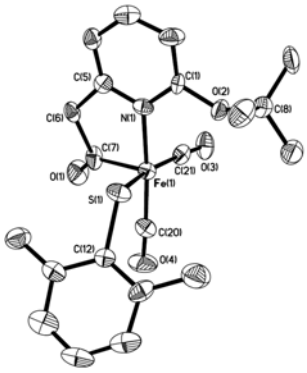

Figure 3. Solid-state structure of **2**. The thermal ellipsoids are displayed at 30 % probability. Selected bond distances (Å) and angle (°): Fe(1)-N(1), 1.953(9); Fe(1)-S(1), 2.219(4); Fe(1)-C(7), 1.827(13); Fe(1)-C(20), 1.773(13); Fe(1)-C(21), 1.761(15); C(20)-O(4), 1.137(14); C(21)-O(3), 1.156(16); C(7)-O(1), 1.220(15); C(21)-Fe(1)-C(20), 90.8(6); C(20)-Fe(1)-N(1), 175.5(5); C(7)-Fe(1)-N(1), 86.3(5); C(21)-Fe(1)-S(1), 163.5(4).

Table 1. Selected Infrared Data.

Complex	ν(CO) (cm^{-1})	Complex	ν(CO) (cm^{-1})
2[a]	2013, 1948	**9a**[b]	2074, 2020, 1989
3[b]	2078, 2027, 2001	**10**[b]	2017, 1956
4[a]	2047, 1988	**11**[b]	2008, 1947
6[a]	2057, 1999	**12**[b]	2006, 1937
6[b]	2065, 2010	**13**[a]	2042, 1972
7[b]	2011, 1944	**13** in CH_2Cl_2	2051, 1986
7a[b]	2063, 2011, 1983	Hmd[c]	1996, 1928
8[a]	2014, 1953	Hmd[d]	2011, 1944
8[b]	2013, 1953	CO-inhibited Hmd[d]	2074, 2020, 1981
9[a]	2024, 1960	Mercaptoethnol-FeGP cofactor[e]	2004, 1934

9[b]	2020, 1956	Mercaptoethnol-FeGP cofactor[d]	2031, 1972
9 in CH_2Cl_2	2022, 1958	Acetic acid-FeGP cofactor[e]	2029, 1957

[a] spectrum of a solid sample on KBr disk. [b] spectrum of a sample dissolved in CH_3CN. [c] spectrum of a solid sample; data from ref. 7. [d] spectrum of a sample dissolved in water; data from ref. 40. [e] spectrum of a solid sample; data from ref. 13.

The ^1H NMR spectrum of **2** in CD_3CN exhibits four signals at 7.97, 7.24-7.20, 7.07 and 6.96 ppm for the pyridyl and phenyl rings, two doublets at 4.44 and 4.04 ppm for the diastereotopic methylene hydrogens, one singlet at 2.30 ppm for the methyl group, and one singlet at 1.58 ppm for the *t*-butoxy group.[38] Monitored by ^1H NMR, no reactivity with H_2 was detected. However, CO could occupy the open position in complex **2**, giving a tricarbonyl complex [2-CH_2CO-6-*t*-BuOC_5H_3N)Fe$(CO)_3${S-(2,6-Me_2-C_6H_3)}] (**3**) (Scheme 2). **3** was characterized by ^1H NMR, ^{13}C NMR and IR spectroscopy. Its ^1H NMR spectrum exhibits two doublets at 5.18 and 4.05 ppm for the diastereotopic methylene hydrogens, and its ^{13}C NMR spectrum shows one signal at 260.9 ppm for acyl carbon, and three signals at 210.3, 208.3 and 205.8 ppm for terminal carbonyl carbons. The IR spectrum of **3** shows three intense ν(CO) absorption bands (Table 1). The third CO ligand in **3** is labile. When a solution of **3** was purged with N_2, **2** was regenerated.

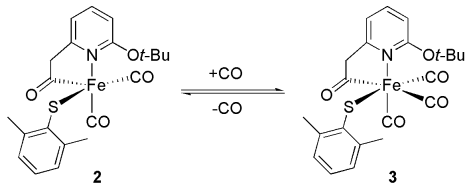

Scheme 3. Reversible reaction of **2** with CO.

Attempts to remove the *t*-Bu group in **2** with Me_3SiI were unsuccessful, and some unidentified species were formed. **2** was also treated with CF_3COOH, but only an ionic product [(2-CH_2CO-6-*t*-BuOC_5H_3N)Fe$(CO)_2(CH_3CN)_2]^+(CF_3COO)^-$ (**4**) was generated in a quantitative yield in CH_3CN (Scheme 4). Complex **4** is not stable in other solvents such as CH_2Cl_2 and THF. The IR spectrum of **4** in the solid state shows two intense ν(CO) absorption bands at 2047 and 1988 cm^{-1} (Table 1), which are comparable with the known ionic complex [(2-CH_2CO-6-$MeOC_5H_3N$)Fe$(CO)_2(CH_3CN)_2]^+(BF_4)^-$,[30] and much higher than that of **2** and [Fe]-hydrogenase. The structure of **4** was further confirmed by ^1H NMR and elemental analysis.

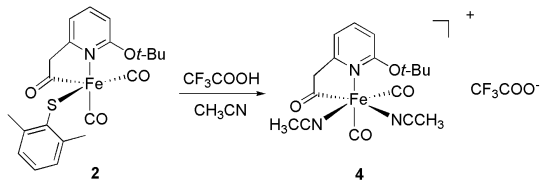

Scheme 4. Reaction of **2** with CF_3COOH.

Iron complexes with acylmethylpyridinol ligand

The difficulty in the deprotection of the *t*-Bu group in complex **2** might be due to the instability of the targeted complex, so we next attempted to deprotect of the *t*-Bu group in the more stable complex **1**. This proved successful. Reaction of **1** with an excess of Me_3SiI (3.5 equiv.), followed by addition of H_2O yielded [(2-CH_2CO-6-HOC_5H_3N)Fe$(CO)_3$I] (**5**) (Scheme 5). In CH_3CN, the IR spectrum of **5** exhibits three ν(CO) absorptions, consistent with its structure.[38] In the solid state, its IR spectrum shows four ν(CO) absorptions, probably due to the same reason proposed for complex **1** (see above).

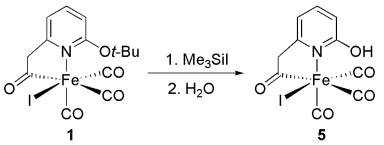

Scheme 5. Synthesis of complex **5**.

The ^1H NMR spectrum of **5** in CD_3CN exhibits one singlet at 10.17 ppm for the hydroxyl group, three signals at 7.81, 7.08 and 6.87 ppm for the pyridyl ring and two doublets at 4.46 and 4.08 ppm for the -CH_2 group. No *t*-Bu group is shown, which is in agreement with the cleavage of the *t*-Bu group.[38]

After the synthesis of **5**, we set out to install a thiolate ligand on the Fe center. Reactions of **5** with PhSNa, (2,6-$Me_2C_6H_3$)SNa, (4-NO_2-C_6H_4)SNa, and C_6F_5SNa did not yield isolable complexes.

An alternative route was developed to synthesize the desired iron thiolate model complexes. Complex **5** was treated with $AgBF_4$ in CH_3CN, giving [(2-CH_2CO-6-HOC_5H_3N)Fe$(CO)_2(CH_3CN)_2]^+(BF_4)^-$ (**6**) (Scheme 6). The two intense ν(CO) absorption bands in its IR spectra (2057 and 1999 cm^{-1} in the solid state; 2065 and 2010 cm^{-1} in CH_3CN) are comparable to that of **4**, and confirm its ionic nature (Table 1). **6** was treated with a series of thiols and thiophenols in the presence of NEt_3 at -30 ^oC to give the targeted thiolate complexes (Scheme 7).

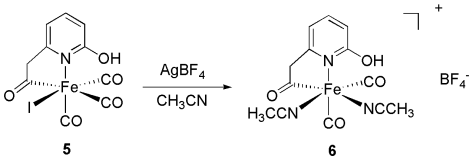

Scheme 6. Synthesis of complex **6**.

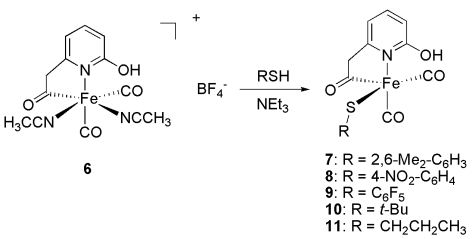

Scheme 7. Synthesis of thiolate iron complexes.

Complexes [(2-CH_2CO-6-HOC_5H_3N)Fe$(CO)_2${S-(2,6-Me_2-C_6H_3)}] (**7**) and [(2-CH_2CO-6-HOC_5H_3N)Fe$(CO)_2${S-(4-NO_2-

C_6H_4)}] (**8**) are highly unstable, and they decomposed completely in 10 mins in the dark at -30 °C. The instability made it impossible to obtain satisfying ^{1}H NMR spectra of these complexes. Their IR spectra in CH_3CN and in the solid state show two intense ν(CO) absorption bands, indicating their existence as monomers both in solution and in the solid state (Table 1).

Complex [(2-CH_2CO-6-HOC_5H_3N)Fe(CO)$_2${S-(C_6F_5)}] (**9**) is much more stable. Its life time is about 1 h at room temperature in the dark. Ambient light accelerates its decomposition (life time is about 30 mins). From the reaction of **6** with C_6F_5SNa, the ^{1}H NMR of **9** could be obtained, although the resolution was not high due to the existence of some paramagnetic impurities. The two characteristic doublets of the diastereotopic methylene hydrogens at 4.66 and 3.91 ppm were evident. The reaction of **9** with x H_2 (1 atomsphere) was monitored by ^{1}H NMR, however, no reaction was found. The result is consistent with the essential role of methenyl-H_4MPT$^+$ for H_2 activation by [Fe]-hydrogenase. It also suggests that replacing the methoxyl group in **2** and its analogues by a hydroxyl group as in **9** does not result in a dramatic change in the reactivity towards H_2.

Like **7** and **8**, complexes [(2-CH_2CO-6-HOC_5H_3N)Fe(CO)$_2$(S-*t*-Bu)] (**10**) and [(2-CH_2CO-6-HOC_5H_3N)Fe(CO)$_2$($SCH_2CH_2CH_3$)] (**11**) could only be identified by IR spectroscopy due to their high instability. From the two intense absorptions (2017 and 1956 cm^{-1} for **10**; 2008 and 1947 cm^{-1} for **11**) (Table 1), both **10** and **11** exist as monomers in CH_3CN. The life time of **10** and **11** is only about 3 mins at -30 °C.

7 and **9** were further selected to study the reactivity with CO. Unexpectedly, upon exposure to CO, the conversion to tricarbonyl products [(2-CH_2CO-6-HOC_5H_3N)Fe(CO)$_3${S-(2,6-Me_2-C_6H_3)}] (**7a**) and [(2-CH_2CO-6-HOC_5H_3N)Fe(CO)$_3${S-(C_6F_5)}] (**9a**) was not complete (33 % for **7** and 38 % for **9**) (Scheme 8).[38] This behavior is different from that of **2** and [Fe]-hydrogenase, which could be completely converted to the tris(carbonyl) complexes.[40] It is worth noting that both the ν(CO) absorption bands of **7a** and **9a** are close to those of CO-inhibited [Fe]-hydrogenase (Table 1).

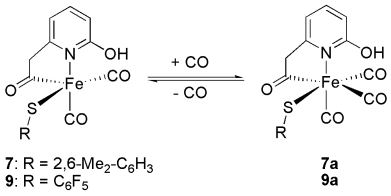

Scheme 8. Reversible reactions of **7** and **9** with CO.

One of the decomposition products of **7** was identified as the tricarbonyl complex **7a** (Figure S12).[38] This decomposition pathway was earlier found for complex [(2-CH_2CO-6-$MeOC_5H_3N$)Fe(CO)$_2${S-(4-NO_2-C_6H_4)}]$_2$.[33] After 2 mins at -30 °C, two new peaks at 2063 and 1983 cm^{-1} appeared, which were attributed to **7a**. After about 10 mins, the decomposition of **7** was complete.[38]

The decomposition reaction of **9** was similar to that of **7**, and **9a** was also formed (Figure S19).[38]

To model the isocyanide- and cyanide-inhibited [Fe]-hydrogenase,[37,40] the reactions of **9** with *p*-toluenesulfonylmethylisocyanide and [NEt_4]CN were explored. Treatment of **9** with *p*-toluenesulfonylmethylisocyanide gave an unstable dicarbonyl product.[38] Treatment of **9** with [NEt_4]CN gave unidentified products. Installation of a 2-mercaptoethanol ligand onto the Fe center was also attempted in order to model the protein-free FeGP cofactor extracted with 2-mercaptoethanol. When **6** was treated with 2-mercaptoethanol in the presence of NEt_3, [(2-CH_2CO-6-HOC_5H_3N)Fe(CO)$_2$(SCH_2CH_2OH)] (**12**) was produced (Scheme 9). The IR spectrum of **12** shows two absorptions at 2006 and 1937 cm^{-1} in CH_3CN, within several cm^{-1} of those of 2-mercaptoethanol extracted FeGP cofactor in the solid state (Table 1). Different from the 5-coordinate models **7** and **9**, **12** did not react with CO, which is similar to the FeGP cofactor extracted with 2-mercaptoethanol.[40] This suggests that **12** is a 6-coordinate complex, with -OH group of 2-mercaptoethanol coordinating to Fe.

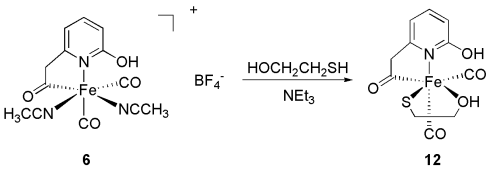

Scheme 9. Synthesis of complex **12**.

Unlike the dinuclear complexes [(2-CH_2CO-6-$MeOC_5H_3N$)Fe(CO)$_2${S-(4-NO_2-C_6H_4)}]$_2$[33] and [(2-CH_2CO-6-$MeOC_5H_3N$)Fe(CO)$_2${SCH_2CH_2OH}]$_2$[31], **7**-**12** all exist as monomers (Table 1). The results demonstrate that the 6-hydroxyl group in the pyridyl ring has certain influences over their structures and possibly activities.

To model the acetic acid extracted FeGP cofactor, acetate ligand was also installed by reacting **5** with CH_3COOAg in CH_2Cl_2 (Scheme 10).

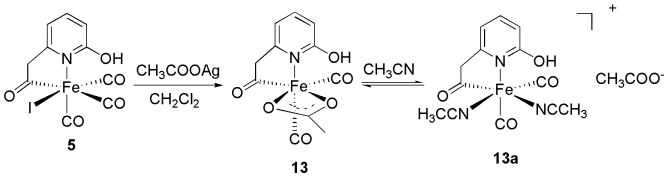

Scheme 10. Reaction of **5** with CH_3COOAg.

The ^{1}H NMR of the product in $CDCl_3$ exhibits three signals at 7.67, 6.86 and 6.68 ppm for the pyridinol ring, two doublets at 4.01 and 3.92 ppm for the -CH_2 group, and one singlet at 2.41 ppm for the acetate group. The IR spectrum displays two intense ν(CO) absorptions both in the solid state and in CH_2Cl_2 (Table 1).[38] The ESI-MS (negative mode) shows an intense peak at 305.9706. All the data are consistent with the formulation of the product as [(2-CH_2CO-6-HOC_5H_3N)Fe(CO)$_2$(CH_3COO)] (**13**) (calculated mass: 305.9701).

Interestingly, two species with a ratio of about 2:1 were detected when **13** was dissolved in CH_3CN, according to the four characteristic peaks at 4.20, 4.05, 3.85 and 3.82 ppm for the -CH_2

groups in CD_3CN. The IR spectrum is also consistent with the ^1H NMR result, and shows four ν(CO) absorption bands.[38] We propose that a second species formed when **13** is dissolved in CH_3CN; this species is $[(2\text{-}CH_2CO\text{-}6\text{-}HOC_5H_3N)Fe(CO)_2(CH_3CN)_2]^+(CH_3COO)^-$ (**13a**) (Scheme 10). A similar transformation was reported for complex $[RuCl_2(tri(pyridylmethyl)amine)]$ in CH_3CN.[41]

Complex **13** could react with C_6F_5SH/NEt_3 to generate **9**. When CH_2Cl_2 was used as the solvent for this reaction, two intense ν(CO) absorptions at 2022 and 1958 cm^{-1} were observed in the IR spectrum of the product, nearly identical to those of **9** produced according to Scheme 7 (Table 1).[38] The reaction of **9** produced from **13** with CH_3CN (20 eq.) was monitored in CH_2Cl_2, but no reaction was found. This result indicates that **9** is 5-coordinate and CH_3CN does not coordinate to Fe, as proposed in Scheme 7.

Similar to $[2\text{-}CH_2CO\text{-}6\text{-}MeOC_5H_3N)Fe(CO)_2\{S\text{-}(2,6\text{-}Me_2\text{-}C_6H_3)\}]$,[30] complexes **7-12** reacted with $HBF_4{\cdot}Et_2O$ to form **6**. This reactivity again suggests that the Cys176 thiolate ligand in [Fe]-hydrogenase might serve as a proton acceptor after H_2 splitting.[30]

Conclusion

In summary, two mononuclear iron complexes with acylmethylpyridinol ligand (**5** and **6**) were synthesized and fully characterized by ^1H NMR, IR and elemental analysis. Starting from **6**, a series of iron thiolate complexes (**7-12**) were generated and identified by IR and/or ^1H NMR (**9**). These complexes are the first mononuclear iron models of [Fe]-hydrogenase that contain an acylmethylpyridinol ligand. Different from the known complexes with 2-acylmethyl-6-methoxy-pyridyl ligand,[31,33] **7-12** always exist as monomers and are not subject to dimerization. This is the evidence that the 6-hydroxyl group in the pyridyl ring can influence the structures and probably the activity of the model complexes. **7-12** reacted with HBF_4 to generate **6**, consistent with the Cys176 thiolate ligand in [Fe]-hydrogenase being a possible proton acceptor after H_2 splitting. An acetate ligand was installed in complex **13**, which serves as a model of the acetic acid extracted FeGP cofactor. The unreactivity of these new models towards H_2 echoes that of [Fe]-hydrogenase, and suggests that methenyl-H_4MPT^+ and the enzymatic environment are essential for H_2 activation.

Experimental Section

Synthesis of $[(2\text{-}CH_2CO\text{-}6\text{-}HOC_5H_3N)Fe(CO)_3I]$ (5)

Me_3SiI (610.0 mg, 3.05 mmol) was added into a solution of **1** (400.0 mg, 0.871 mmol) in CH_2Cl_2 (10 mL) under stirring at room temperature. After 12 h, H_2O (20 mL) was added into the mixture. The water phase was washed with CH_2Cl_2 (20 mL × 3) and ether (10 mL), respectively. The combined organic phase was washed with H_2O (20 mL). After drying the organic phase over Na_2SO_4 and evaporation of the solvent, the residue was extracted with ether (10 mL), and the filtrate was dried in vacuum. The residue was washed with hexane (40 mL) and CH_2Cl_2 (1 mL), respectively. The solid residue was then extracted with ether (10 mL) again, and the filtrate was dried in vacuum. The residue was washed with hexane (20 mL) and recrystallized from ether/hexane to afford **5** (110.0 mg, 0.273 mmol; yield: 31 %) as a red solid.

^1H NMR (400.13 MHz, CD_3CN): 10.17 (s, 1H), 7.81(t, *J = 8.0 Hz*, 1H), 7.08 (d, *J = 8.0 Hz*, 1H), 6.87 (d, *J = 8.0 Hz*, 1H), 4.46 (d, *J = 20.0* Hz, 1H), 4.08 (d, *J = 20.0* Hz, 1H) ppm. IR (ν_{CO}, KBr, cm^{-1}): 2102 (s), 2048 (s), 2023 (s), 2014 (s). IR (ν_{CO}, CH_3CN, cm^{-1}): 2068 (s), 2050 (s), 1996 (s). Anal. Calcd for $C_{10}H_6FeNO_5I$: C, 29.8; H, 1.5; N, 3.5. Found: C, 30.1; H, 1.5, N, 3.8.

Synthesis of $[(2\text{-}CH_2CO\text{-}6\text{-}HOC_5H_3N)Fe(CO)_2(CH_3CN)_2]^+(BF_4)^-$ (6)

$AgBF_4$ (48.1 mg, 0.248 mmol) was added into a solution of **5** (100.0 mg, 0.248 mmol) in CH_3CN (5 mL) under stirring. Gas (CO) was formed immediately. After 1 min, the mixture was filtered and the filtrate was dried in vacuum. The residue was washed with ether (10 mL) and dried in vacuum to afford **6** (101.0 mg, 0.242 mmol; 98 %) as a light yellow oily solid.

^1H NMR (400.13 MHz, CD_3CN): 9.33 (s, 1H), 7.83 (t, *J = 8.0 Hz*, 1H), 7.10 (d, *J = 8.0 Hz*, 1H), 6.88 (d, *J = 8.0 Hz*, 1H), 4.66 (d, *J = 20.0 Hz*, 1H), 3.89 (d, *J = 20.0 Hz*, 1H), 1.96 (s, 6H) ppm. IR (ν_{CO}, KBr, cm^{-1}): 2057 (s), 1999 (s). IR (ν_{CO}, CH_3CN, cm^{-1}): 2065 (s), 2010 (s). Anal. Calcd for $C_{13}H_{12}BF_4FeN_3O_4$: C, 37.5; H, 2.9; N, 10.1. Found: C, 37.7; H, 3.0, N, 9.9.

General procedure to the synthesis of thiolate complexes 7-12

Thiol or thiophenol (0.048~0.096 mmol, 1~2 eq.) was added into a solution of **6** (20.0 mg, 0.048 mmol) in CH_3CN (5 mL) under stirring. NEt_3 (0.048~0.096 mmol, 1~2 eq.) was added into the mixture at -30 °C. The IR spectrum was recorded immediately. If $HBF_4{\cdot}Et_2O$ (0.048~0.14 mmol, 1~3 eq.) was added quickly after the formation of the thiolate product, **6** was regenerated.

Acknowledgements

This work was supported by the National Natural Science Foundation of China (Nos. 21242012, 21201049, and 21302028), Harbin Science and Technology Bureau (2013RFLXJ002), the Fundamental Research Funds for the Central Universities (Grant No. HIT. NSRIF. 2013042), and the Swiss National Science Foundation (Project no. 200020_134473/1).

[1] S. Shima, R. K. Thauer, *Chem. Rec.* **2007**, *7*, 37-46.

[2] S. Shima, R. K. Thauer, U. Ermler, *Met. Ions Life Sci.* **2009**, *6*, 219-240.

[3] F. Gloaguen, T. B. Rauchfuss, *Chem. Soc. Rev.* **2009**, *38*, 100-108.

[4] M. Y. Darensbourg, *Comments Inorg. Chem.* **2010**, *31*, 144-152.

[5] M. T. Stiebritz, M. Reiher, *Chem. Sci.* **2012**, *3*, 1739-1751.

[6] S. Shima, O. Pilak, S. Vogt, M. Schick, M. S. Stagni, W. Meyer-Klaucke, E. Warkentin, R. K. Thauer, U. Ermler, *Science* **2008**, *321*, 572-575.

[7] T. Hiromoto, K. Ataka, O. Pilak, S. Vogt, M. S. Stagni, W. Meyer-Klaucke, E. Warkentin, R. K. Thauer, S. Shima, U. Ermler, *FEBS Lett.* **2009**, *583*, 585-590.

[8] T. Hiromoto, E. Warkentin, J. Moll, U. Ermler, S. Shima, *Angew. Chem.* **2009**, *121*, 6579-6582; *Angew. Chem., Int. Ed.* **2009**, *48*, 6457-6460.

[9] E. J. Lyon, S. Shima, G. Buurman, S. Chowdhuri, A. Batschauer, K. Steinbach, R. K. Thauer, *Eur. J. Biochem.* **2004**, *271*, 195-204.

[10] S. Shima, E. J. Lyon, M. S. Sordel-Klippert, M. Kauss, J. Kahnt, R. K. Thauer, K. Steinbach, X. L. Xie, L. Verdier, C. Griesinger, *Angew. Chem.* **2004**, *116*, 2601-2605; *Angew. Chem., Int. Ed.* **2004**, *43*, 2547-2551.

[11] S. Shima, U. Ermler, *Eur. J. Inorg. Chem.* **2011**, 963-972.

[12] M. Schick, X. Xie, K. Ataka, J. Kahnt, U. Linne, S. Shima, *J. Am. Chem. Soc.* **2012**, *134*, 3271-3280.

[13] S. Shima, M. Schick, J. Kahnt, K. Ataka, K. Steinbach, U. Linne, *Dalton Trans.* **2012**, *41*, 767-771.

[14] C. Tard, C. J. Pickett, *Chem. Rev.* **2009**, *109*, 2245-2274.

[15] J. A. Wright, P. J. Turrell, C. J. Pickett, *Organometallics* **2010**, *29*, 6146-6156.

[16] M. J. Corr, J. A. Murphy, *Chem. Soc. Rev.* **2010**, *40*, 2279-2292.

[17] S. Dey, P. K. Das, A. Dey, *Coord. Chem. Rev.* **2013**, *257*, 42-63.

[18] K. M. Schultz, D. Chen, X. Hu, *Chem. Asian J.* **2013**, *8*, 1068-1075.

[19] A. M. Royer, T. B. Rauchfuss, D. L. Gray, *Organometallics* **2009**, *28*, 3618-3620.

[20] B. V. Obrist, D. Chen, A. Ahrens, V. Schunemann, R. Scopelliti, X. Hu, *Inorg. Chem.* **2009**, *48*, 3514-3516.

[21] B. Li, T. Liu, C. V. Popescu, A. Bilko, M. Y. Darensbourg, *Inorg. Chem.* **2009**, *48*, 11283–11289.

[22] T. B. Liu, B. Li, C. V. Popescu, A. Bilko, L. M. Perez, M. B. Hall, M. Y. Darensbourg, *Chem.-Eur. J.* **2010**, *16*, 3083-3089.

[23] S. Tanino, Y. Ohki, K. Tatsumi, *Chem. Asian. J.* **2010**, *5*, 1962-1964.

[24] P. J. Turrell, J. A. Wright, J. N. T. Peck, V. S. Oganesyan, C. J. Pickett, *Angew. Chem.* **2010**, *122*, 7670-7673; *Angew. Chem., Int. Ed.* **2010**, *49*, 7508-7511.

[25] A. M. Royer, M. Salomone-Stagni, T. B. Rauchfuss, W. Meyer-Klaucke, *J. Am. Chem. Soc.* **2010**, *132*, 16997-17003.

[26] D. Chen, R. Scopelliti, X. Hu, *J. Am. Chem. Soc.* **2010**, *132*, 928-929.

[27] D. Chen, R. Scopelliti, X. Hu, *Angew. Chem.* **2010**, *122*, 7674-7677; *Angew. Chem., Int. Ed.* **2010**, *49*, 7512-7515.

[28] D. Chen, R. Scopelliti, X. Hu, *Angew. Chem.* **2011**, *123*, 5789-5791; *Angew. Chem., Int. Ed.* **2011**, *50*, 5670-5672.

[29] D. Chen, A. Ahrens-Botzong, V. Schuemann, R. Scopelliti, X. Hu, *Inorg. Chem.* **2011**, *50*, 5249-5257.

[30] D. Chen, R. Scopelliti, X. Hu, *Angew. Chem.* **2012**, *124*, 1955-1957; *Angew. Chem., Int. Ed.* **2012**, *51*, 1919-1921.

[31] B. Hu, D. Chen, X. Hu. *Chem. Eur. J.* **2012**, *18*, 11528-11530.

[32] L.-C. Song, Z.-J. Xie, M.-M. Wang, G.-Y. Zhao, H.-B. Song, *Inorg. Chem.* **2012**, *51*, 7466-7468.

[33] B. Hu, D. Chen, X. Hu, *Chem. Eur. J.* **2013**, *19*, 6221-6224.

[34] P. J. Turrell, A. D. Hill, S. K. Ibrahim, J. A. Wright, C. J. Pickett, *Dalton Trans.* **2013**, *42*, 8140-8146.

[35] L.-C. Song, G.-Y. Zhao, Z.-J. Xie, J.-W. Zhang, *Organometallics* **2013**, *32*, 2509-2512.

[36] X. Yang, M. B. Hall. *J. Am. Chem. Soc.* **2009**, *131*, 10901-10908.

[37] H. Tamura, M. Salomone-Stagni, T. Fujishiro, E. Warkentin, W. Meyer-Klaucke, U. Ermler, S. Shima, *Angew. Chem.* **2013**, *125*, 9838-9841; *Angew. Chem. Int. Ed.* **2013**, *52*, 9656-9659.

[38] See supporting information.

[39] Y. Guo, H. Wang, Y. Xiao, S. Vogt, R. K. Thauer, S. Shima, P. I. Volkers, T. B. Rauchfuss, V. Pelmenschikov, D. A. Case, E. E. Alp, W. Sturhahn, Y. Yoda, S. P. Cramer, *Inorg. Chem.* **2008**, *47*, 3969-3977.

[40] E. J. Lyon, S. Shima, R. Boecher, R. K. Thauer, F. W. Grevels, E. Bill, W. Roseboom, S. P. J. Albracht. *J. Am. Chem. Soc.* **2004**, *126*, 14239.

[41] C. J. Whiteoak, J. D. Nobbs, E. Kiryushchenkov, S. Pagano, A. J. P. White, G. J. P. Britovsek, *Inorg. Chem.* **2013**, *52*, 7000-7009.

Received: ((will be filled in by the editorial staff))
Revised: ((will be filled in by the editorial staff))
Published online: ((will be filled in by the editorial staff))

Entry for the Table of Contents (Please choose one layout only)

Layout 2:

Bio-Mimetic Chemistry

Bowen Hu, Dafa Chen, and Xile Hu* ……..… Page – Page

Synthesis and Reactivity of Mononuclear Iron Models of [Fe]-Hydrogenase that Contain an Acylmethylpyridinol Ligand

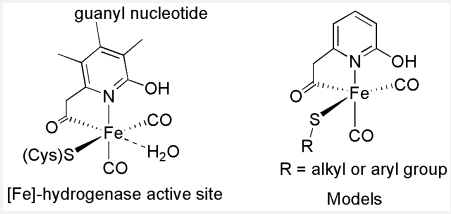

A series of 5-coordinate thiolate iron complexes that precisely modeled the active site of [Fe]-hydrogenase were synthesized. These complexes are first mononuclear models with acylmethylpyridinol ligand.

Supporting Information

Synthesis and Reactivity of Mononuclear Iron Models of [Fe]-Hydrogenase that Contain an Acylmethylpyridinol Ligand

Bowen Hu, Dafa Chen, and Xile Hu*

Dr. B. Hu, Prof. Dr. D. Chen
School of Chemical Engineering & Technology, Harbin Institute of Technology, Harbin 150001, P. R. China.
E-mail: dafachen@hit.edu.cn

Prof. Dr. X. Hu
Laboratory of Inorganic Synthesis and Catalysis, Institute of Chemical Sciences and Engineering, Ecole Polytechnique Fédérale de Lausanne (EPFL), SB-ISIC-LSCI, BCH 3305, Lausanne 1015, Switzerland.
E-mail: xile.hu@epfl.ch

Experimental Section

A. Chemicals and Reagents

All manipulations were carried out under an inert N_2(g) atmosphere using a Schlenk line. Solvents were distilled from appropriate drying agents under N_2 before use. All reagents were purchased from commercial sources. Liquid compounds were degassed by standard freeze-pump-thaw procedures prior to use. 2-*tert*-butoxy-6-chloropyridine was prepared as described previously.[S1]

B. Physical methods

The ^{1}H and ^{13}C NMR spectra were recorded on a Bruker Avance 400 spectrometer. ^{1}H NMR chemical shifts were referenced to residual solvent as determined relative to Me_4Si ($\delta = 0$ ppm). The $^{13}C\{^1H\}$ chemical shifts were reported in ppm relative to the carbon resonance of $CDCl_3$ (77.0 ppm). IR spectra were recorded on a Nicolet iS5 FT-IR spectrometer. Elemental analyses were performed on a Perkin-Elmer 240C analyzer. Mass spectra were performed on an Agilent 6530 Accurate-Mass Quadrupole Time-of-Flight (Q-TOF) mass spectrometer, equipped with an ESI source. X-ray diffraction studies were carried out in a Xcalibur E X-ray single crystal diffractometer. Data collections were performed using four-circle kappa diffractometers equipped with CCD detectors. Data were reduced and then corrected for absorption.[S2] Solution, refinement and geometrical calculations for all crystal structures were performed by SHELXTL.[S3]

C. Synthetic methods

Synthesis of 2-*tert*-butoxy-6-methylpyridine

2-*tert*-butoxy-6-methylpyridine was prepared using a similar method as described previously.[S1] A solution of CH_3MgBr/ether (3 M, 10.8 mL, 32.4 mmol) was added drop-wise to a mixture of 2-*tert*-butoxy-6-chloropyridine (4.0 g, 21.6 mmol) and 1,2-bis(diphenylphosphino)ethane nickel(II) chloride (34.2 mg, 0.0648 mmol) in THF (40 mL). The mixture was stirred at room temperature for 4 h. The reaction was diluted with ether (20 mL) and quenched by addition of H_2O to dissolve inorganics. The organic phase was washed with H_2O. After drying the organic phase over Na_2SO_4 and evaporation of the solvent, the crude products were purified by silica gel column chromatography, giving 2-*tert*-butoxy-6-methylpyridine as a colorless oil (2.79 g, 16.9 mmol; yield 78 %).

^{1}H NMR (400.13 MHz, $CDCl_3$): 7.41 (t, *J = 7.6 Hz*, 1H), 6.67 (d, *J = 7.6 Hz*, 1H), 6.47 (d, *J = 7.6 Hz*, 1H), 2.43 (s, 3H), 1.57 (s, 9H) ppm. ^{13}C NMR (400.13 MHz, $CDCl_3$): 163.2, 155.7, 138.3, 115.2, 109.7, 79.1, 28.7, 24.2. MS (ESI, positive mode): Calcd for $C_{10}H_{15}NO$ + H: 166.1232. Found: 166.1223. Anal. Calcd for $C_{10}H_{15}NO$: C, 72.7; H, 9.2; N, 8.5. Found: C, 73.0; H, 9.1, N, 8.2.

Synthesis of [(2-CH_2CO-6-*t*-$BuOC_5H_3N$)$Fe(CO)_3I$] (**1**)

n-BuLi (5 mL, 1.6 M, 8.0 mmol) was added into a solution of 2-*tert*-butoxy-6-methylpyridine (1.32 g, 8.0 mmol) in THF (50 mL) under stirring at 0 °C. After stirring for 0.5 h at this temperature, the solution was added into a solution of $Fe(CO)_5$ (1.57 g, 8.0 mmol) in THF (50

mL) at -50 °C, and the resulting solution was warmed slowly to -20 °C (about 2 h). The solution was then cooled to -60 °C, followed by adding solid I_2 (2.03 g, 8.0 mmol) at the same temperature. The resulting solution was kept at -60 °C for 2 hours. The solvent was then evaporated in vacuum. The residue was placed in an Al_2O_3 column. Elution with CH_2Cl_2 developed a red band, which afforded **1** (1.87 g, 4.1 mmol; yield: 51 %) as red crystals after recrystallization from CH_2Cl_2/ether.

^{1}H NMR (400.13 MHz, $CDCl_3$): 7.73 (t, *J = 8.0 Hz*, 1H), 7.11 (d, *J = 8.0 Hz*, 1H), 6.99 (d, *J = 8.0 Hz*, 1H), 5.42 (d, *J = 20.0 Hz*, 1H), 4.29 (d, *J = 20.0 Hz*, 1H), 1.70 (s, 9H) ppm. IR ($\nu_{CO,}$ KBr, cm^{-1}): 2089 (s), 2045 (s), 2034 (s), 2011 (s), 2000 (s). IR ($\nu_{CO,}$ CH_2Cl_2, cm^{-1}): 2088 (s), 2040 (s), 2008 (s). Anal. Calcd for $C_{14}H_{14}FeINO_5$: C, 36.6; H, 3.1; N, 3.1. Found: C, 36.7; H, 3.1, N, 2.9.

Synthesis of [2-CH_2CO-6-*t*-BuOC_5H_3N)Fe$(CO)_2${S-(2,6-Me_2-C_6H_3)}] (**2**)

A newly synthesized sample of (2,6-Me_2-C_6H_3)SNa (228.0 mg, 1.38 mmol), which was prepared by NaH (33.2 mg, 1.38 mmol) and (2,6-Me_2-C_6H_3)SH (190.6 mg, 1.38 mmol) in THF, was mixed with complex **1** (634.0 mg, 1.38 mmol) in CH_2Cl_2 (10 mL). After stirring for 0.5 h at room temperature in the dark, the solvent was evaporated in vacuum. The residue was extracted with CH_2Cl_2 (4 mL). After removing the solvent of the filtrate, the residue was recrystallized from CH_2Cl_2/hexane at -30 °C in the dark to afford **2** (430.0 mg, 0.975 mmol; yield: 71 %) as red crystals.

^{1}H NMR (400.13 MHz, CD_3CN): 7.97 (t, *J = 8.0 Hz*, 1H), 7.24-7.20 (m, 2H), 7.07 (d, *J = 8.0 Hz*, 2H), 6.96 (d, *J = 8.0 Hz*, 1H), 4.44 (d, *J = 20.0* Hz, 1H), 4.04 (d, *J = 20.0* Hz, 1H), 2.30 (s, 6H), 1.58 (s, 9H) ppm. IR (ν_{CO}, KBr, cm^{-1}): 2013 (s), 1948 (s). Anal. Calcd for $C_{21}H_{23}FeNO_4S$: C, 57.2; H, 5.3; N, 3.2. Found: C, 57.5; H, 5.4, N, 3.4.

Reaction of **2** with CO: Formation of [(2-CH_2CO-6-*t*-BuOC_5H_3N)Fe$(CO)_3${S-(2,6-Me_2-C_6H_3)}] (**3**)

A solution of **2** (20 mg, 0.045 mmol) in 0.5 mL $CDCl_3$ was added to a J Young NMR tube. The solution was frozen and the tube was evacuated under vacuum. 1 atm of CO was added and the tube was sealed. The color changed from red to yellow as soon as the solution was thawed. The NMR and IR showed [(6-*t*-BuO-C_5H_3N-2-CH_2CO)Fe$(CO)_3${S-(2,6-Me_2-C_6H_3)}] (**3**) formed. If the tube was opened and flushed with N_2, **3** would transform back to **2**.

^{1}H NMR (400.13 MHz, $CDCl_3$): 7.72 (br s, 1H), 7.12-6.90 (m, 5H), 5.18 (d, *J = 20.0* Hz, 1H), 4.05 (d, *J = 20.0* Hz, 1H), 2.19 (s, 6H), 1.63 (s, 9H) ppm. ^{13}C NMR (400.13 MHz, $CDCl_3$): 260.9 (CH_2***C***O), 210.3 (terminal ***C***O), 208.3 (terminal ***C***O), 205.8 (terminal ***C***O), 163.6, 161.5, 144.3, 141.7, 139.6, 127.2, 125.0, 114.9, 108.6, 84.4, 66.0, 28.7, 22.4. ppm. IR (ν_{CO}, CH_3CN, cm^{-1}): 2078 (s), 2027 (s), 2001 (s).

Synthesis of [(2-CH_2CO-6-*t*-BuOC_5H_3N)Fe$(CO)_2(CH_3CN)_2]^+(CF_3COO)^-$ (**4**)

CF_3COOH (25.9 mg, 0.227 mmol) was added into a solution of **2** (100.0 mg, 0.227 mmol) in CH_3CN (2 mL) under stirring at room temperature. The color changed from red to yellow immediately. After 1 min, the solvent was evaporated. The solid residue was washed with Et_2O (10 mL) and dried in vacuum. Compound **4** was isolated as a yellow solid in a quantitative yield (113.2 mg, 0.227 mmol). Attempts to remove the *t*-Bu group with excess of CF_3COOH were failed.

^{1}H NMR (400.13 MHz, CD_3CN): 7.84 (t, *J = 8.0 Hz*, 1H), 7.11 (d, *J = 8.0 Hz*, 2H), 4.62 (d, *J = 20.0* Hz, 1H), 3.66 (d, *J = 20.0* Hz, 1H), 1.94 (s, 6H), 1.62 (s, 9H) ppm. IR (ν_{CO}, KBr, cm^{-1}): 2047 (s), 1988 (s). Anal. Calcd for $C_{19}H_{20}F_3FeN_3O_6$: C, 45.7; H, 4.0; N, 8.4. Found: C, 45.9; H, 4.1, N, 8.7.

Synthesis of [(2-CH_2CO-6-HOC_5H_3N)$Fe(CO)_3I$] (**5**)

Me_3SiI (610.0 mg, 3.05 mmol) was added into a solution of **1** (400.0 mg, 0.871 mmol) in CH_2Cl_2 (10 mL) under stirring at room temperature. After 12 h, H_2O (20 mL) was added into the mixture. The water phase was washed with CH_2Cl_2 (20 mL × 3) and ether (10 mL), respectively. The combined organic phase was washed with H_2O (20 mL). After drying over Na_2SO_4 and evaporation of the solvent, the residue was extracted with ether (10 mL), and the filtrate was dried in vacuum. The residue was washed with hexane (40 mL) and CH_2Cl_2 (1 mL), respectively. The solid residue was then extracted with ether (10 mL) again, and the filtrate was dried in vacuum. The residue was washed with hexane (20 mL) and recrystallized from ether/hexane to afford **5** (110.0 mg, 0.273 mmol; yield: 31 %) as a red solid.

^{1}H NMR (400.13 MHz, CD_3CN): 10.17 (s, 1H), 7.81(t, *J = 8.0 Hz*, 1H), 7.08 (d, *J = 8.0 Hz*, 1H), 6.87 (d, *J = 8.0 Hz*, 1H), 4.46 (d, *J = 20.0* Hz, 1H), 4.08 (d, *J = 20.0* Hz, 1H) ppm. IR (ν_{CO}, KBr, cm^{-1}): 2102 (s), 2048 (s), 2023 (s), 2014 (s). IR ($\nu_{CO,}$ CH_3CN, cm^{-1}): 2068 (s), 2050 (s), 1996 (s). Anal. Calcd for $C_{10}H_6FeNO_5I$: C, 29.8; H, 1.5; N, 3.5. Found: C, 30.1; H, 1.5, N, 3.8.

Synthesis of [(2-CH_2CO-6-HOC_5H_3N)$Fe(CO)_2(CH_3CN)_2]^+(BF_4)^-$ (**6**)

$AgBF_4$ (48.1 mg, 0.248 mmol) was added into a solution of **5** (100.0 mg, 0.248 mmol) in CH_3CN (5 mL) under stirring. Gas (CO) was formed immediately. After 1 min, the mixture was filtered and the filtrate was dried in vacuum. The residue was washed with ether (10 mL) and dried in vacuum to afford **6** (101.0 mg, 0.242 mmol; 98 %) as a light yellow oily solid.

^{1}H NMR (400.13 MHz, CD_3CN): 9.33 (s, 1H), 7.83 (t, *J = 8.0 Hz*, 1H), 7.10 (d, *J = 8.0 Hz*, 1H), 6.88 (d, *J = 8.0 Hz*, 1H), 4.66 (d, *J = 20.0 Hz*, 1H), 3.89 (d, *J = 20.0 Hz*, 1H), 1.96 (s, 6H) ppm. IR ($\nu_{CO,}$ KBr, cm^{-1}): 2057 (s), 1999 (s). IR ($\nu_{CO,}$ CH_3CN, cm^{-1}): 2065 (s), 2010 (s). Anal. Calcd for $C_{13}H_{12}BF_4FeN_3O_4$: C, 37.5; H, 2.9; N, 10.1. Found: C, 37.7; H, 3.0, N, 9.9.

Reaction of **6** with HS-(2,6-Me_2-C_6H_3) and NEt_3: Synthesis of [(2-CH_2CO-6-HOC_5H_3N)$Fe(CO)_2${S-(2,6-Me_2-C_6H_3)}] (**7**)

HS-(2,6-Me_2-C_6H_3) (6.62~13.2 mg, 0.048~0.096 mmol) was added into a solution of **6** (20.0 mg, 0.048 mmol) in CH_3CN (5 mL) under stirring. NEt_3 (4.85~9.79 mg, 0.048~0.096 mmol) was added into the mixture at -30 ^oC. The color changed from light yellow to red immediately. The IR spectrum was recorded immediately, showing two intense *ν*(CO) absorption bands at 2011 and 1944 cm^{-1}. The intensity of the two bands decreased quickly, with the emergence of two new bands at 2063 and 1983 cm^{-1}. After about 10 mins, almost all the bands between 2100-1900 cm^{-1} disappeared, and the color changed to black.

If $HBF_4{\cdot}Et_2O$ (7.77 mg~23.3 mg, 0.048~0.14 mmol) was added quickly after the formation of **7**, **6** was regenerated.

IR ($\nu_{CO,}$ CH_3CN, cm^{-1}): 2011 (s), 1944 (s).

Reaction of **7** with CO: Formation [(2-CH_2CO-6-HOC_5H_3N)$Fe(CO)_3${S-(2,6-Me_2-C_6H_3)}] (**7a**)

HS-(2,6-Me_2-C_6H_3) (6.62~13.2 mg, 0.048~0.096 mmol) was added into a solution of **6** (20.0 mg, 0.048 mmol) in CH_3CN (5 mL) under CO atmosphere. NEt_3 (4.85~9.79 mg, 0.048~0.096

mmol) was added into the mixture at -30 °C. The color changed from light yellow to red immediately. The IR spectrum was recorded immediately, showing four *v*(CO) absorption bands at 2063, 2011, 1983 and 1944 cm^{-1}. The intensity of the peak at 2063 cm^{-1} is about 50 % of that of the peak at 1944 cm^{-1}, indicating that about 33 % of **7** transformed to **7a**.

7a: IR ($\nu_{CO,}$ CH_3CN, cm^{-1}): 2063 (s), 2011 (s), 1983 (s).

Reaction of **6** with HS-(4-NO_2-C_6H_4) and NEt_3: Synthesis of [(2-CH_2CO-6-HOC_5H_3N)$Fe(CO)_2${S-(4-NO_2-C_6H_4)}] (**8**)

HS-(4-NO_2-C_6H_4) (7.43~14.9 mg, 0.048~0.096 mmol) was added into a solution of **6** (20.0 mg, 0.048 mmol) in CH_3CN (5 mL) under stirring. NEt_3 (4.85~9.79 mg, 0.048~0.096 mmol) was added into the mixture at -30 °C. The color changed from light yellow to red immediately. The IR spectrum was recorded immediately, showing two intense *v*(CO) absorption bands at 2013 and 1953 cm^{-1}. The intensity of the two bands decreased quickly, with the emergence of two new bands at 2071 and 1992 cm^{-1}. After about 10 mins, almost all the bands between 2100-1900 cm^{-1} disappeared, and the color changed to black.

If $HBF_4 \cdot Et_2O$ (7.77 mg~23.3 mg, 0.048~0.14 mmol) was added quickly after the formation of **8**, **6** was regenerated.

IR ($\nu_{CO,}$ solid, cm^{-1}): 2014 (s), 1953 (s). IR ($\nu_{CO,}$ CH_3CN, cm^{-1}): 2013 (s), 1953 (s).

Reaction of **6** with HS-(C_6F_5) and NEt_3: Synthesis of [(2-CH_2CO-6-HOC_5H_3N)$Fe(CO)_2${S-(C_6F_5)}] (**9**)

HS-(C_6F_5) (9.59~19.2 mg, 0.048~0.096 mmol) was added into a solution of **6** (20.0 mg, 0.048 mmol) in CH_3CN (5 mL) under stirring. NEt_3 (4.85~9.79 mg, 0.048~0.096 mmol) was added into the mixture at -30 °C. The color changed from light yellow to deep yellow immediately. The IR spectrum was recorded immediately, showing two intense *v*(CO) absorption bands at 2020 and 1956 cm^{-1}. The intensity of the two bands decreased with the time, and two new bands at 2074 and 1989 cm^{-1} appeared. After about 1 h, almost all the bands between 2100-1900 cm^{-1} disappeared, and the color changed to black.

If $HBF_4 \cdot Et_2O$ (7.77 mg~23.3 mg, 0.048~0.14 mmol) was added quickly after the formation of **9**, **6** was regenerated.

IR ($\nu_{CO,}$ solid, cm^{-1}): 2024 (s), 1960 (s). IR ($\nu_{CO,}$ CH_3CN, cm^{-1}): 2020 (s), 1956 (s).

Reaction of **6** with NaS-(C_6F_5): An alternative route to synthesize **9**

NaS-(C_6F_5) (2.66 mg, 0.012 mmol) was added into a solution of **6** (5.00 mg, 0.012 mmol) in CD_3CN (0.6 mL) in a J Young NMR tube at -30 °C. The ^1H NMR was measured immediately, which showed **9** formed. Some precipitate can be found in the tube after the ^1H NMR measurement.

^1H NMR (400.13 MHz, CD_3CN): 7.73 (br s, 1H), 6.98-6.71 (m, 2H), 4.37 (d, *J = 20.0 Hz*, 1H), 3.91 (d, *J = 20.0 Hz*, 1H) ppm.

Reaction of **9** with CO: Formation of [(2-CH_2CO-6-HOC_5H_3N)$Fe(CO)_3${S-(C_6F_5)}] (**9a**)

HS-(C_6F_5) (9.59~19.2 mg, 0.048~0.096 mmol) was added into a solution of **6** (20.0 mg, 0.048 mmol) in CH_3CN (5 mL) under a CO atmosphere. NEt_3 (4.85~9.79 mg, 0.048~0.096 mmol) was added into the mixture at -30 °C. The IR spectrum was recorded immediately, showing four *v*(CO) absorption bands at 2074, 2020, 1989 and 1956 cm^{-1}. The intensity of the peak at 2074

cm^{-1} is about 60 % of that of the peak at 1956 cm^{-1}, showing that about 38 % of **9** transformed to **9a**.

9a: IR ($\nu_{CO,}$ CH_3CN, cm^{-1}): 2074 (s), 2020 (s), 1989 (s).

Reaction of **9** with *p*-toluenesulfonylmethylisocyanide

HS-(C_6F_5) (9.59~19.2 mg, 0.048~0.096 mmol) was added into a solution of **6** (20.0 mg, 0.048 mmol) in CH_3CN (5 mL). NEt_3 (4.85~9.79 mg, 0.048~0.096 mmol) and *p*-toluenesulfonylmethylisocyanide (9.36~18.7 mg, 0.048~0.096 mmol) were added into the mixture at -30 ^oC, respectively. The IR spectrum was recorded immediately, showing two *v*(CO) absorption bands at 2027 and 1974 cm^{-1}. The product decomposed completely in 15 mins at room temperature in the dark.

Reaction of **6** with *t*-BuSH and NEt_3: Synthesis of [(2-CH_2CO-6-HOC_5H_3N)Fe$(CO)_2$(S-*t*-Bu)] (**10**)

t-BuSH (4.32~8.64 mg, 0.048~0.096 mmol) was added into a solution of **6** (20.0 mg, 0.048 mmol) in CH_3CN (5 mL) under stirring. NEt_3 (4.85~9.79 mg, 0.048~0.096 mmol) was added into the mixture at -30 ^oC. The color changed from light yellow to red immediately. The IR spectrum was recorded immediately, showing two intense *v*(CO) absorption bands at 2017 and 1956 cm^{-1}. The intensity of the two bands decreased quickly, with the emergence of two new bands at 2061 and 1978m $^{-1}$. After about 3 mins, almost all the bands between 2100-1900 cm^{-1} disappeared, and the color changed to black.

If $HBF_4{\cdot}Et_2O$ (7.77 mg~23.3 mg, 0.048~0.14 mmol) was added quickly after the formation of **10**, **6** was regenerated.

IR ($\nu_{CO,}$ CH_3CN, cm^{-1}): 2017 (s), 1956 (s).

Reaction of **6** with $CH_3CH_2CH_2SH$ and NEt_3: Synthesis of [(2-CH_2CO-6-HOC_5H_3N)Fe$(CO)_2$($SCH_2CH_2CH_3$)] (**11**)

$CH_3CH_2CH_2SH$ (3.65~7.30 mg, 0.048~0.096 mmol) was added into a solution of **6** (20.0 mg, 0.048 mmol) in CH_3CN (5 mL) under stirring. NEt_3 (4.85~9.79 mg, 0.048~0.096 mmol) was added into the mixture at -30 ^oC. The color changed from light yellow to red immediately. The IR spectrum was recorded immediately, showing two intense *v*(CO) absorption bands at 2008 and 1947 cm^{-1}. After about 3 mins, almost all the bands between 2100-1900 cm^{-1} disappeared, and the color changed to black.

If $HBF_4{\cdot}Et_2O$ (7.77 mg~23.3 mg, 0.048~0.14 mmol) was added quickly after the formation of **11**, **6** was regenerated.

IR ($\nu_{CO,}$ CH_3CN, cm^{-1}): 2008 (s), 1947 (s).

Reaction of **6** with $HOCH_2CH_2SH$ and NEt_3: Synthesis of [(2-CH_2CO-6-HOC_5H_3N)Fe$(CO)_2$(SCH_2CH_2OH)] (**12**)

$HOCH_2CH_2SH$ (3.74~7.48 mg, 0.048~0.096 mmol) was added into a solution of **6** (20.0 mg, 0.048 mmol) in CH_3CN (5 mL) under stirring. NEt_3 (4.85~9.79 mg, 0.048~0.096 mmol) was added into the mixture at -30 ^oC. The color changed from light yellow to red immediately. The IR spectrum was recorded immediately, showing two intense *v*(CO) absorption bands at 2006 and 1937 cm^{-1}. After about 10 mins, almost all the bands between 2100-1900 cm^{-1} disappeared, and the color changed to black.

IR ($\nu_{CO,}$ CH_3CN, cm^{-1}): 2006 (s), 1937 (s).

Reaction of **5** with CH_3COOAg: Synthesis of [(2-CH_2CO-6-HOC_5H_3N)Fe$(CO)_2(CH_3COO)$] (**13**) and/or [(2-CH_2CO-6-HOC_5H_3N)Fe$(CO)_2(CH_3CN)_2]^+(CH_3COO)^-$ (**13a**)

CH_3COOAg (41.2 mg, 0.248 mmol) was added into a solution of **5** (50.0 mg, 0.124 mmol) in CH_2Cl_2 (5 mL) under stirring. Gas (CO) was formed immediately. After 5 mins, the mixture was filtered and the filtrate was dried in vacuum. The residue was washed with ether (10 mL) and dried in vacuum to afford **13** (35.0 mg, 0.114 mmol, 92 %) as yellow oily solid. When dissolved in CH_3CN, parts of **13** transformed to **13a**.

13: ^{1}H NMR (400.13 MHz, $CDCl_3$): 7.67 (t, *J = 8.0 Hz*, 1H), 6.86 (d, *J = 8.0 Hz*, 1H), 6.68 (d, *J = 8.0 Hz*, 1H), 4.01 (d, *J = 20.0 Hz*, 1H), 3.92 (d, *J = 20.0 Hz*, 1H), 2.41 (s, 3H) ppm. IR ($\nu_{CO,}$ solid, cm^{-1}): 2042 (s), 1972 (s). IR ($\nu_{CO,}$ CH_2, cm^{-1}): 2051 (s), 1986 (s). MS (ESI, negative mode): Calcd for $C_{11}H_9FeNO_6$ - H: 305.9701. Found: 305.9706. Anal. Calcd for $C_{11}H_9NFeO_6$: C, 43.0; H, 3.0; N, 4.6. Found: C, 42.7; H, 3.2, N, 4.3.

Mixture of **13** and **13a**: ^{1}H NMR (400.13 MHz, CD_3CN): 7.73 (t, *J = 8.0 Hz*, 1H), 6.90 (d, *J = 8.0 Hz*, 1H), 6.65 (d, *J = 8.0 Hz*, 1H), [4.20 (d, *J = 20.0 Hz*), 4.05 (d, *J = 20.0 Hz*) (1H in total)], [3.85 (d, *J = 20.0 Hz*), 3.82 (d, *J = 20.0 Hz*) (1H in total)], 1.96 (m) ppm. IR ($\nu_{CO,}$ CH_3CN, cm^{-1}): 2054 (s), 2044 (sh), 1994 (s), 1979 (sh).

Reaction of **13** with HS-(C_6F_5) and NEt_3: An alternative route to synthesize **9**

HS-(C_6F_5) (13.0~26.0 mg, 0.065~0.130 mmol) was added into a solution of **13** (20.0 mg, 0.065 mmol) in CH_2Cl_2 (5 mL) under stirring. NEt_3 (6.57~13.1 mg, 0.065~0.130 mmol) was added into the mixture at -30 ^oC. The IR spectrum was recorded immediately, showing two intense *v*(CO) absorption bands at 2022 and 1958 cm^{-1}. CH_3CN (53.3 mg, 0.65 mmol) was then added to the solution, and there was no change of the *v*(CO) absorptions, which meant that CH_3CN did not coordinate with Fe center.

D. Crystallographic Details for 2

A total of 4644 reflections ($-12 \le h \le 12$, $-13 \le k \le 8$, $-12 \le l \le 11$) were collected at $T = 293(2)$ K in the range of 2.94 to 25^o of which 2898 were unique ($R_{int} = 0.0395$); $Mo_{K\square}$ radiation (λ = 0.71073 Å). The structure was solved by the direct methods. All non-hydrogen atoms were refined anisotropically, and hydrogen atoms were placed in calculated idealized positions. The residual peak and hole electron densities were 1.520 and –0.542 eA^{-3}, respectively. The least squares refinement converged normally with residuals of $R(F) = 0.0898$, $wR(F^2) = 0.2337$ and a GOF = 1.098 ($I>2\sigma(I)$). $C_{21}H_{23}FeNO_4S$, Mw = 441.31, space group *P*2(1), Monoclinic, a = 10.2510(18), b = 11.4645(10), c = 10.414(2) Å, β = 114.51(2) °, V = 1113.6(3) $Å^3$, $Z = 2$, ρ_{calcd} = 1.316 Mg/m^3. CCDC 963961 contains the supplementary crystallographic data for this paper. These data can be obtained free of charge from The Cambridge Crystallographic Data Centre via www.ccdc.cam.ac.uk/data_request/cif.

References

(S1)Hintermann, L.; Dang, T. T.; Labonne, A.; Kribber, T.; Xiao, L.; Naumov, P. *Chem. Eur. J.* **2009**, *15*, 7167-7179.

(S2)Blessing, R. H. *Acta Crystallogr. A* **1995**, *51*, 33-38.

(S3)Sheldrick, G. M. *SHELXTL* release 6.1.4 ed.; Bruker AXS Inc.: Madison, Wisconsin, 53719, USA, 2003.

IR spectra

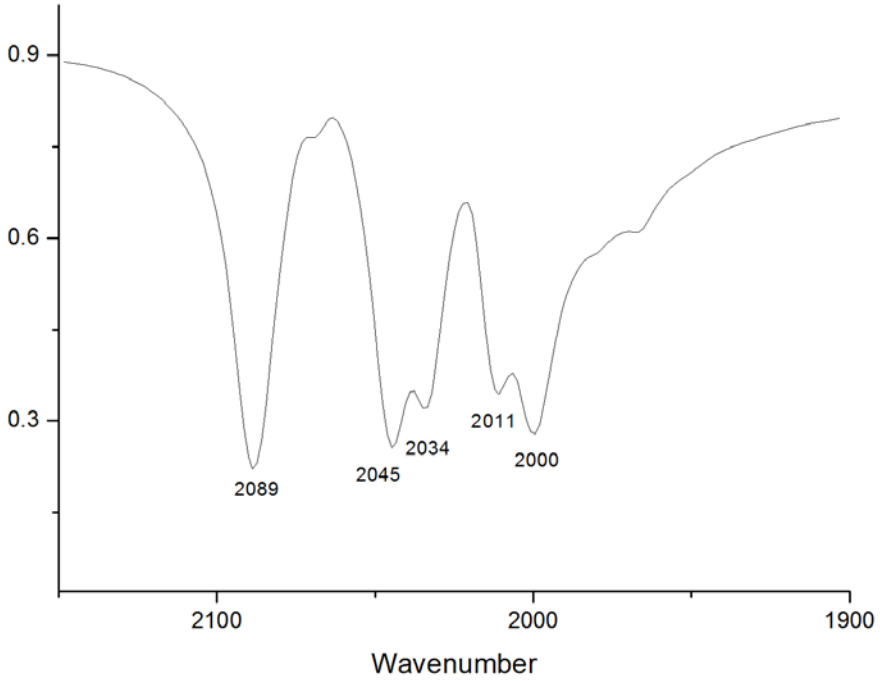

Figure S1. IR spectrum of **1** in the solid state.

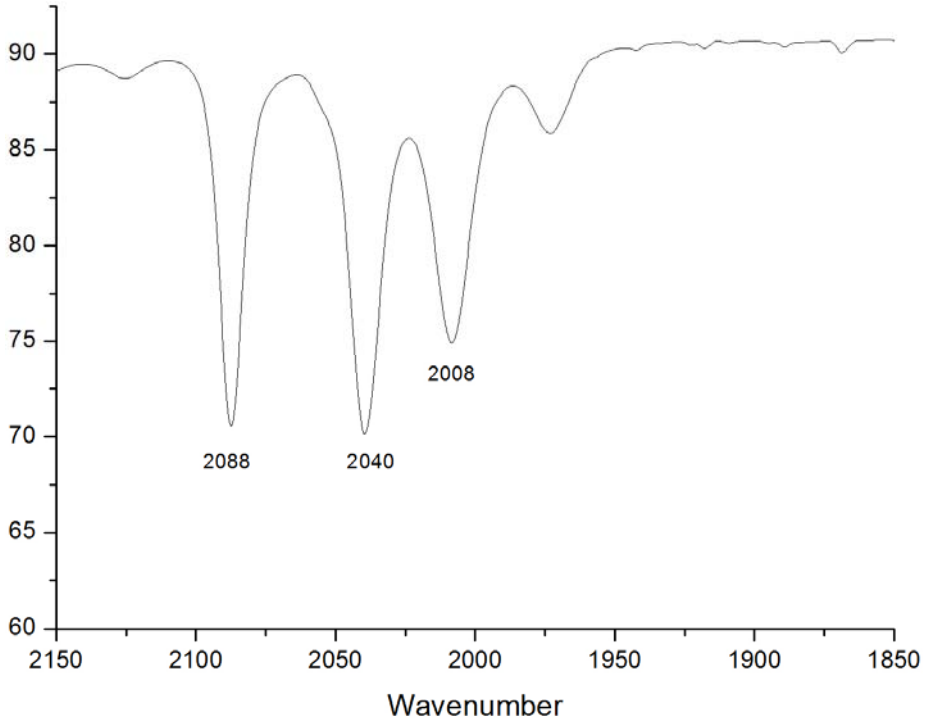

Figure S2. IR spectrum of **1** in CH_2Cl_2.

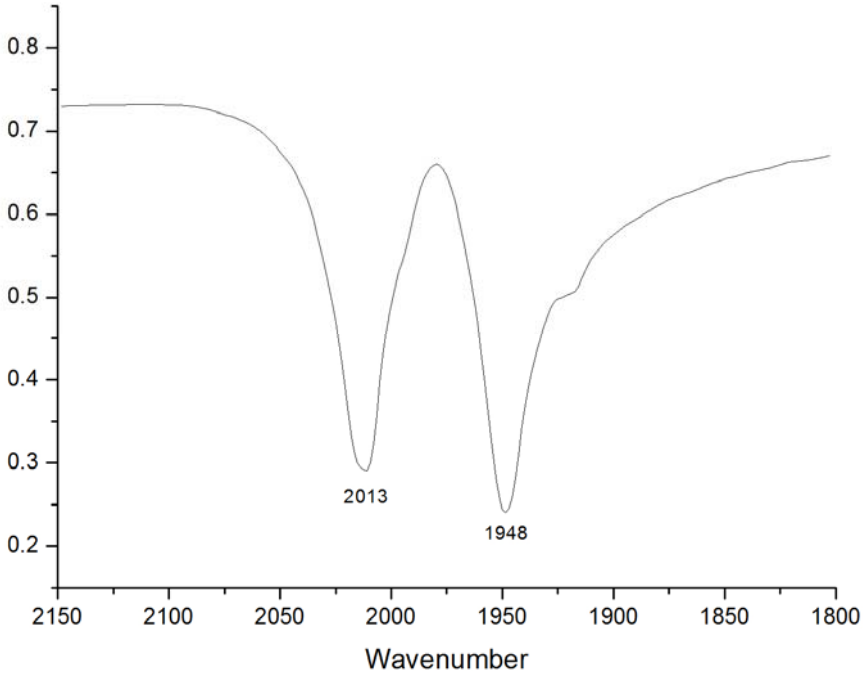

Figure S3. IR spectrum of **2** in the solid state.

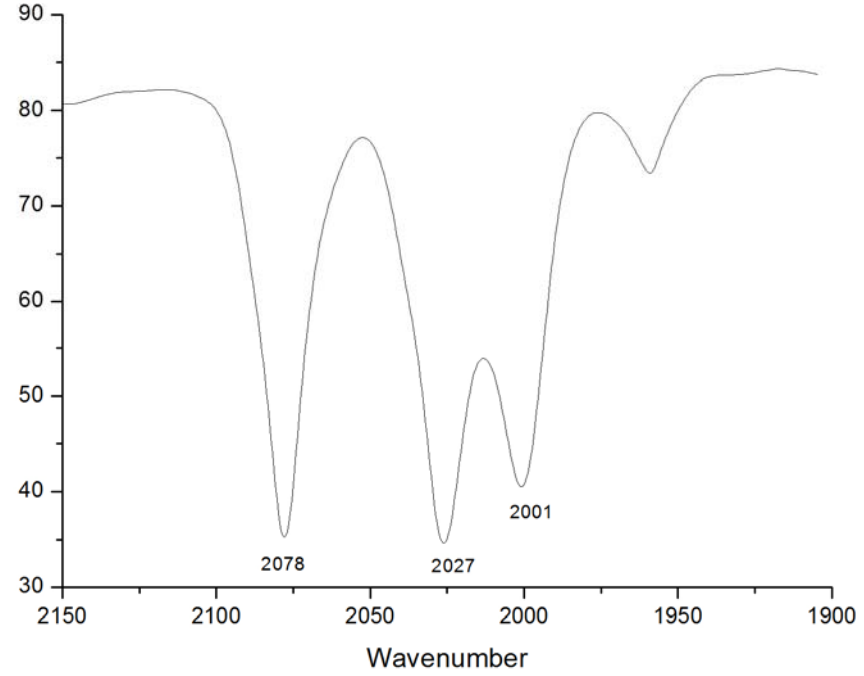

Figure S4. IR spectrum of **3** in CH_3CN.

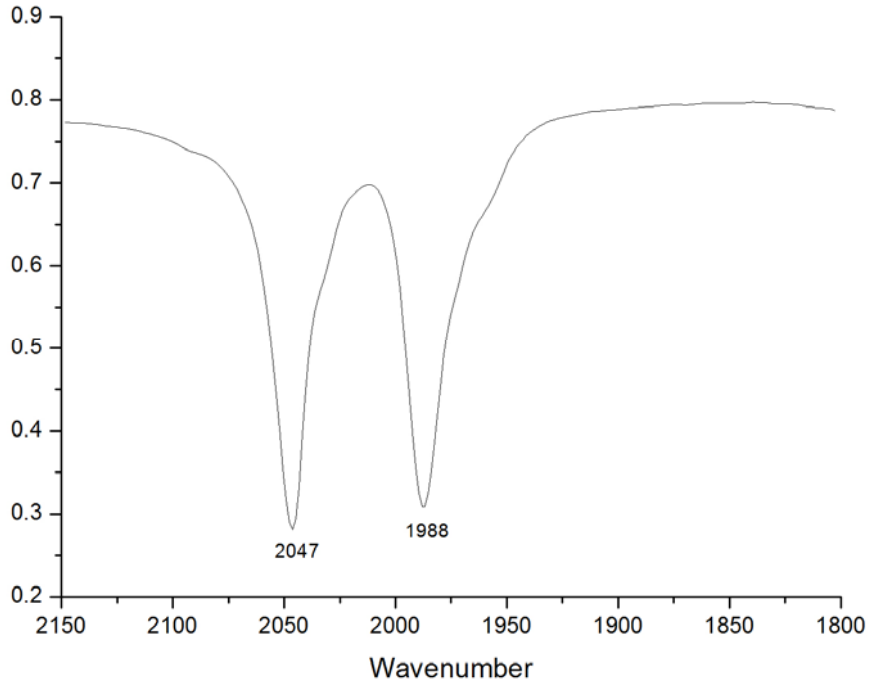

Figure S5. IR spectrum of **4** in the solid state.

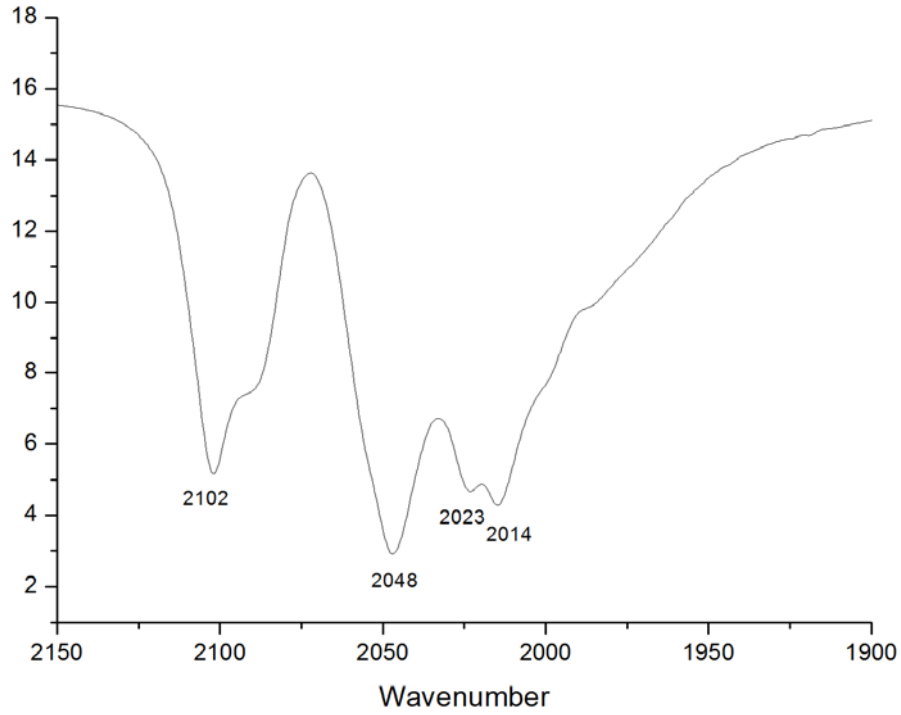

Figure S6. IR spectrum of **5** in the solid state.

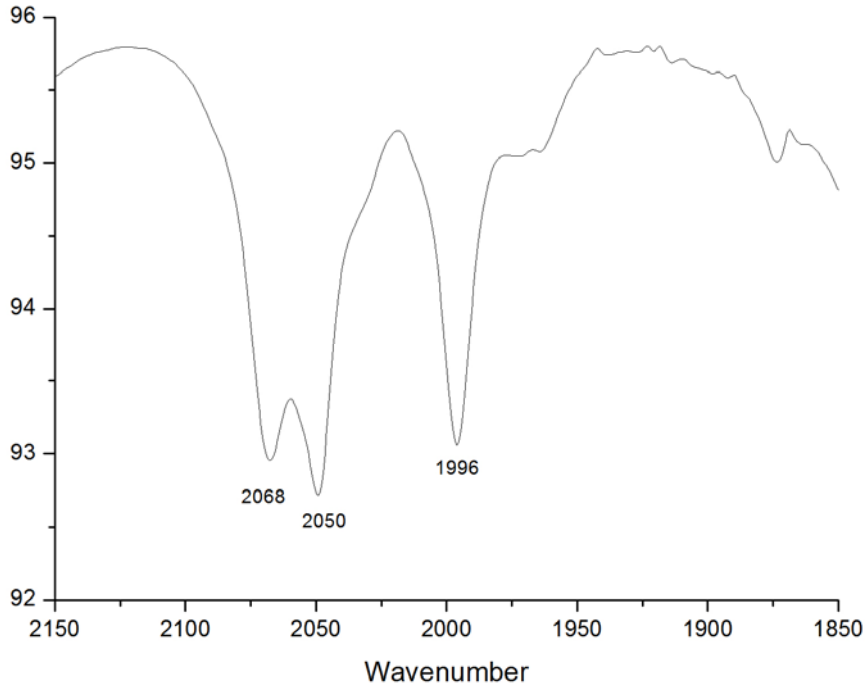

Figure S7. IR spectrum of **5** in CH_3CN.

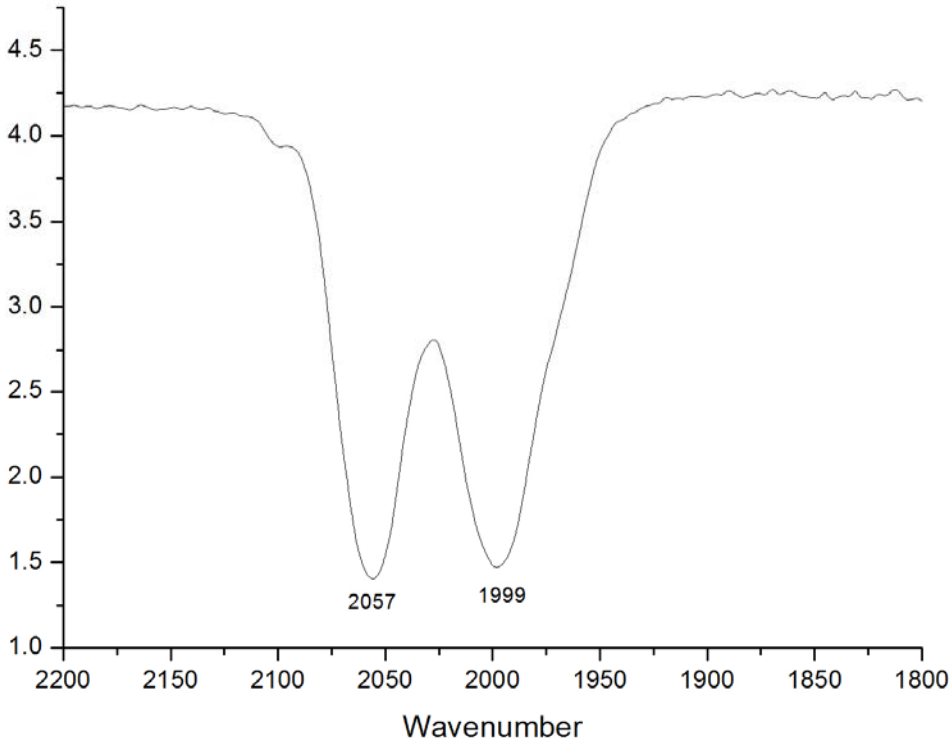

Figure S8. IR spectrum of **6** in the solid state.

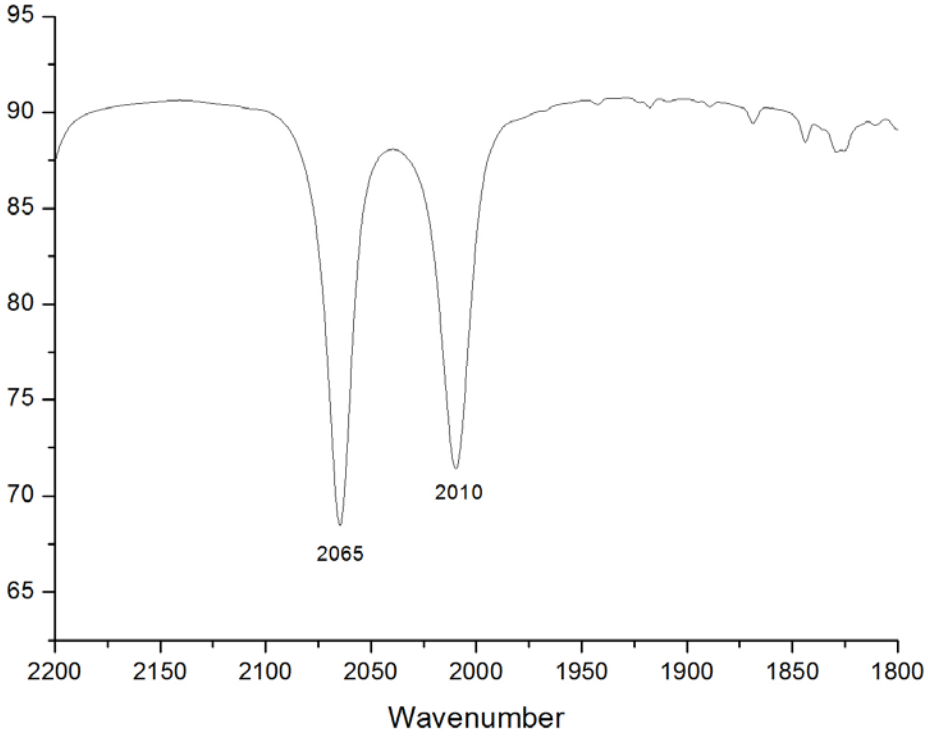

Figure S9. IR spectrum of **6** in CH_3CN.

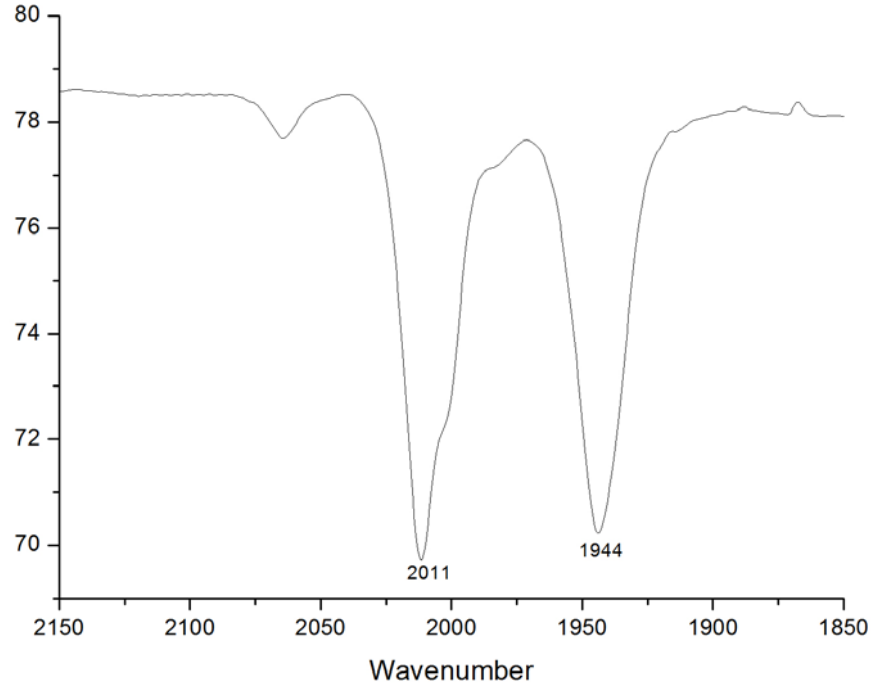

Figure S10 IR spectrum of **7** in CH_3CN.

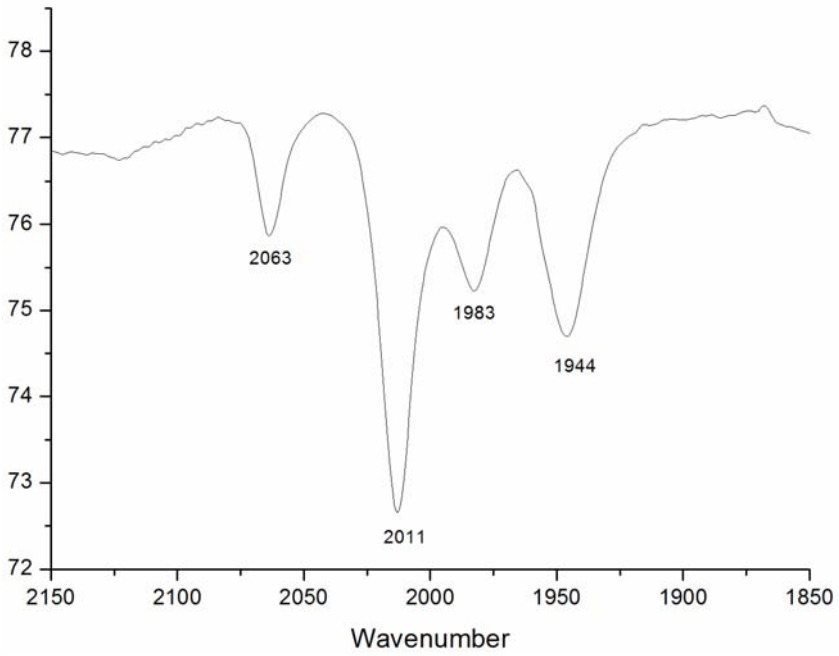

Figure S11. Reaction of **7** with CO

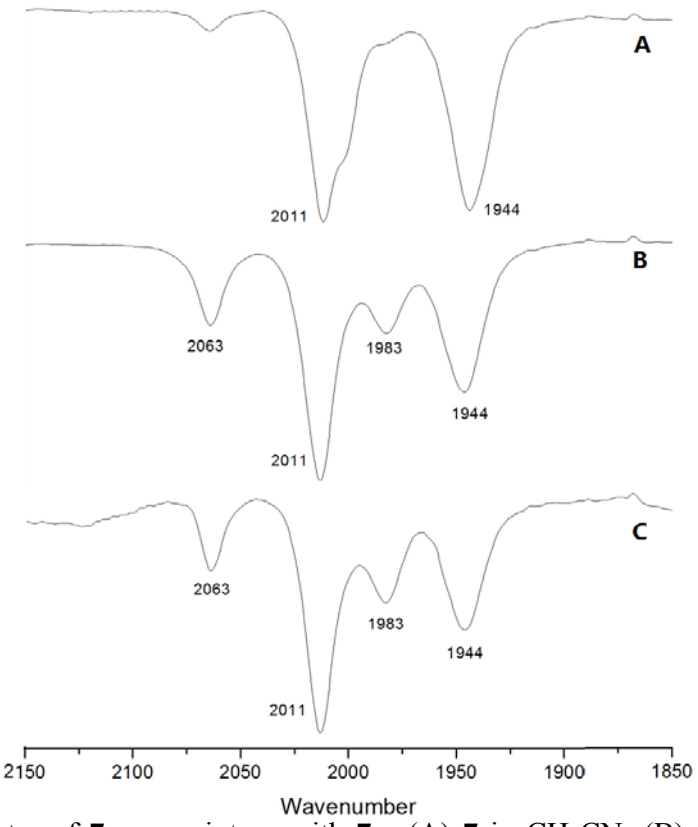

Figure S12. IR spectra of **7** or a mixture with **7a**: (A) **7** in CH_3CN; (B) 2 mins later of **7** in CH_3CN at -30 ^oC; (C) **7** in the presence of CO (a mixture of **7** and **7a**).

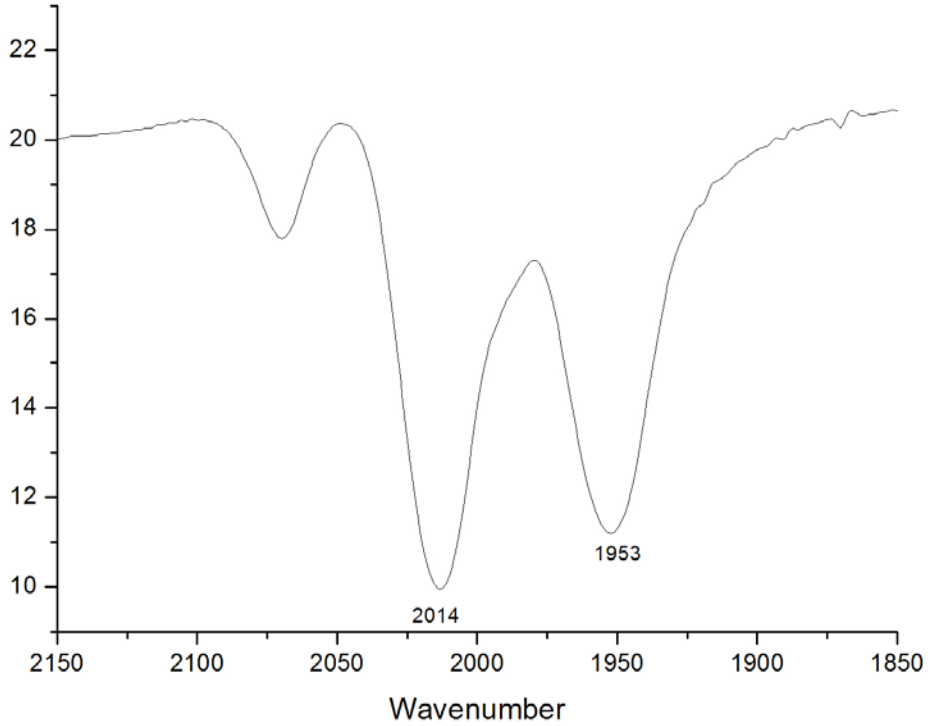

Figure S13. IR spectrum of **8** in the solid state.

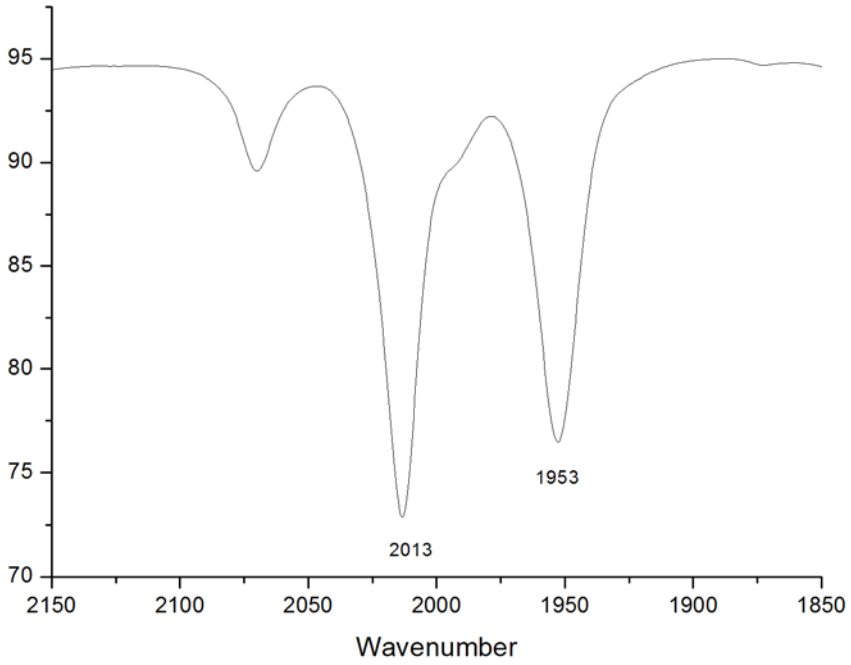

Figure S14. IR spectrum of **8** in CH_3CN.

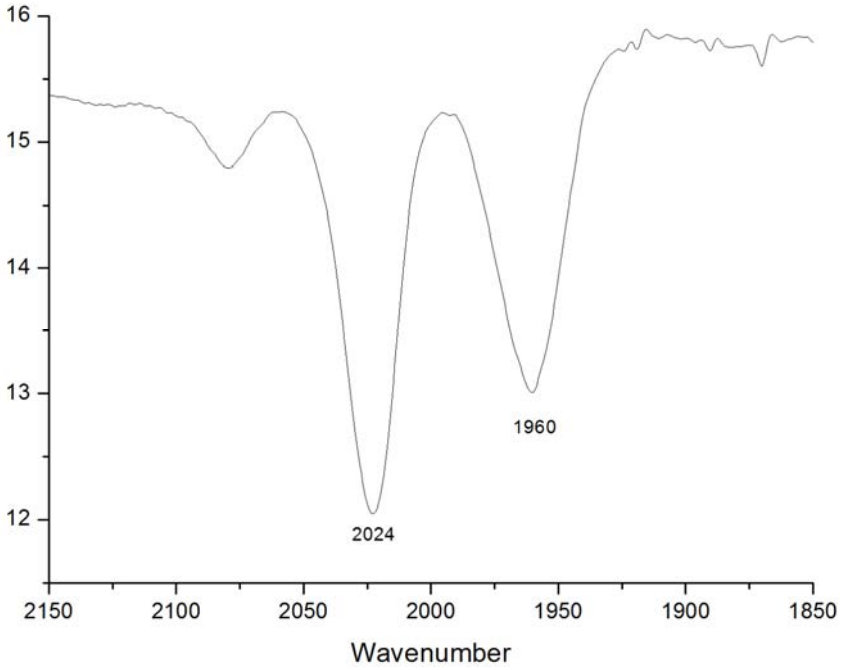

Figure S15. IR spectrum of **9** in the solid state.

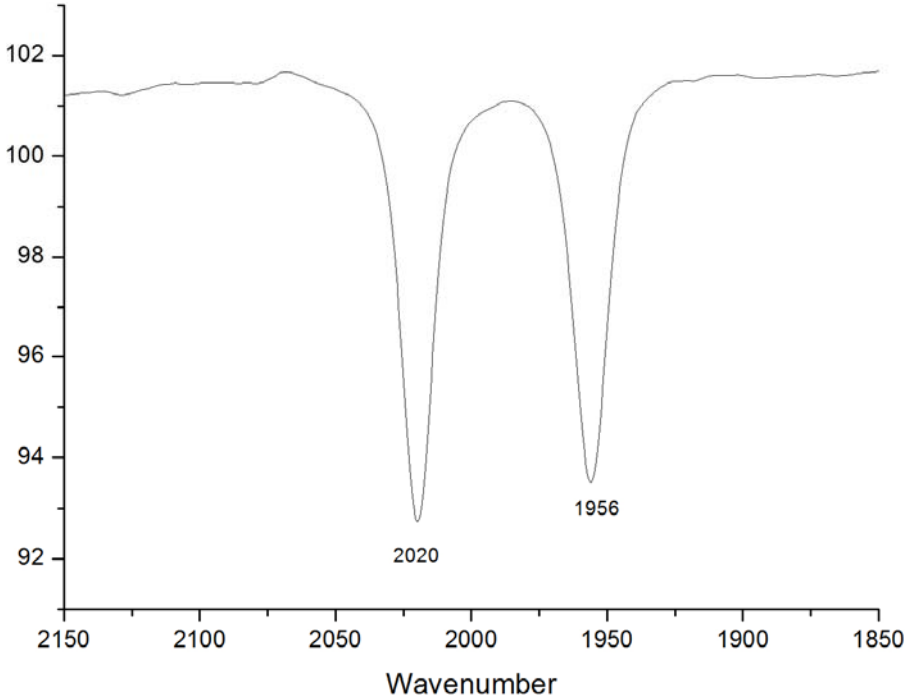

Figure S16. IR spectrum of **9** in CH_3CN.

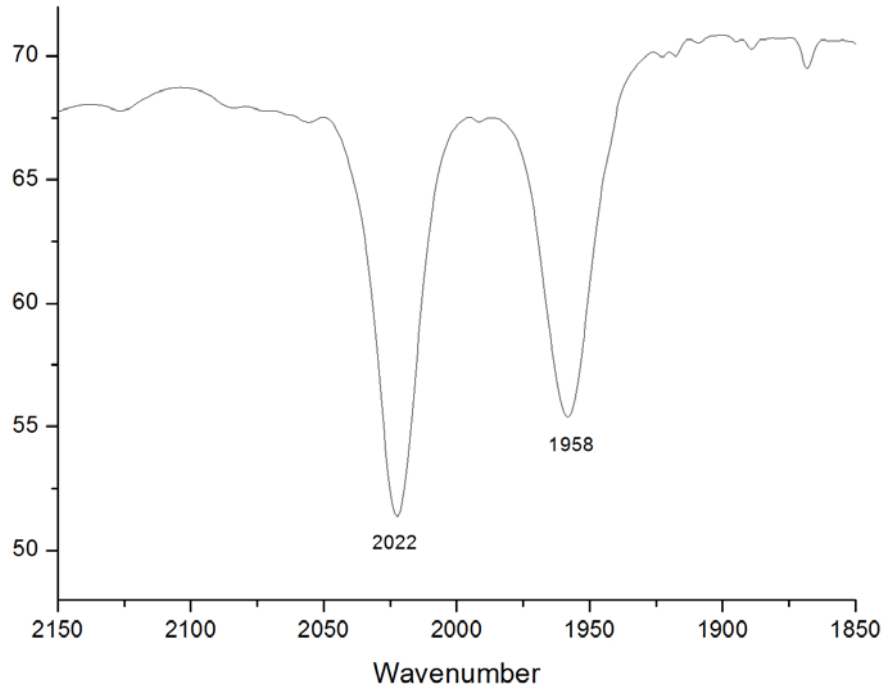

Figure S17. IR spectrum of **9** in CH_2Cl_2.

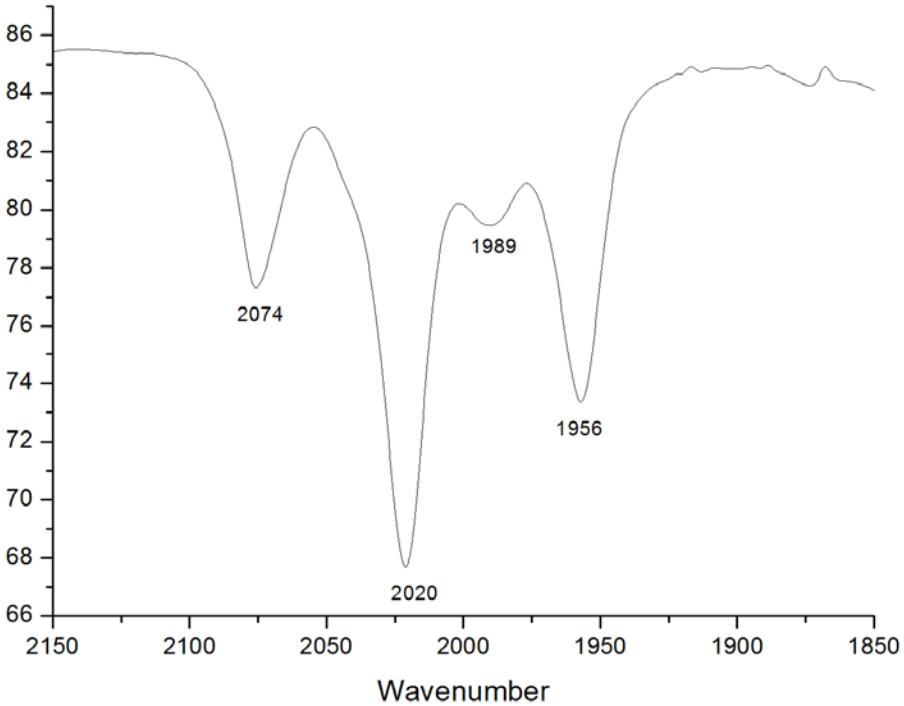

Figure S18. Reaction of **9** with CO.

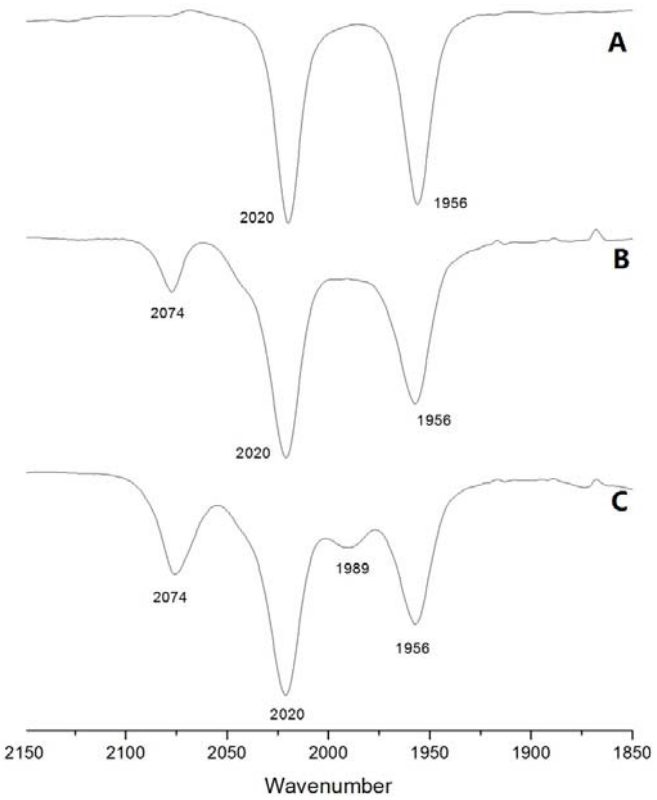

Figure S19. IR spectra of **9** or a mixture with **9a**: (A) **9** in CH_3CN; (B) 20 mins later of **9** in CH_3CN at room temperature; (C) **9** in the presence of CO (a mixture of **9** and **9a**).

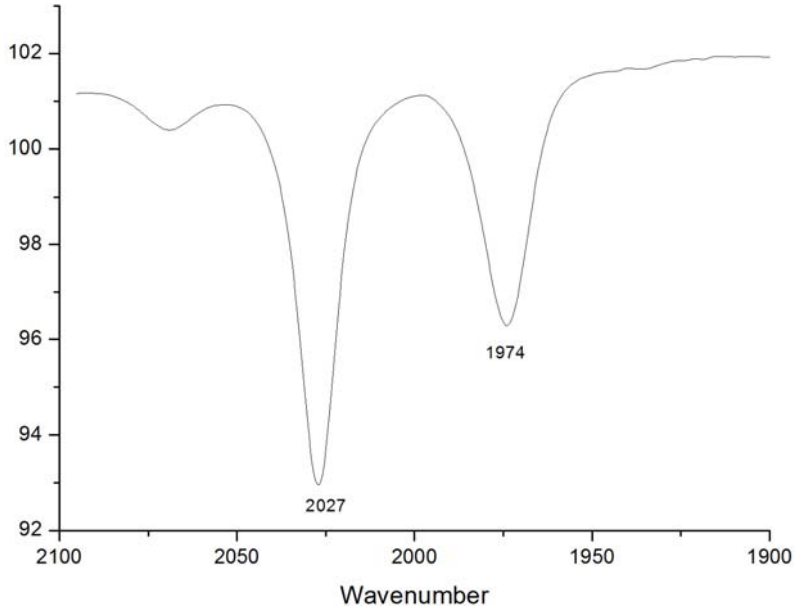

Figure S20. Reaction of **9** with *p*-toluenesulfonylmethylisocyanide in CH_3CN.

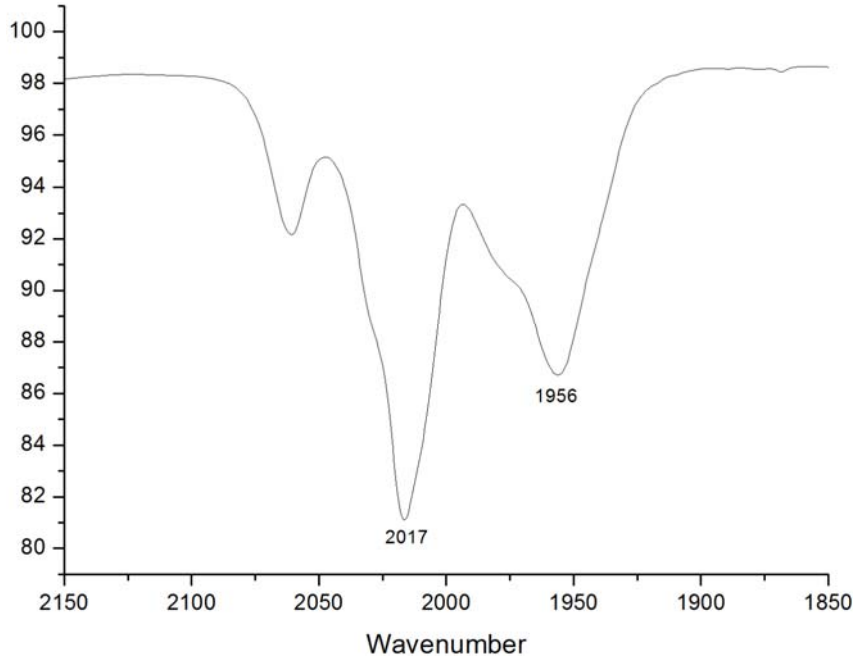

Figure S21. IR spectrum of **10** in CH_3CN.

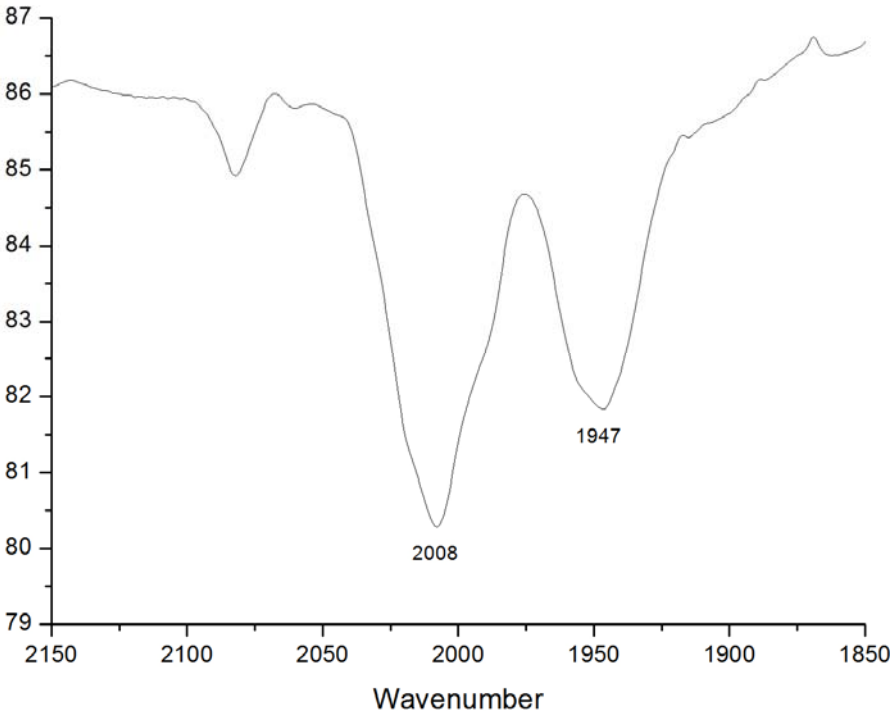

Figure S22. IR spectrum of **11** in CH_3CN.

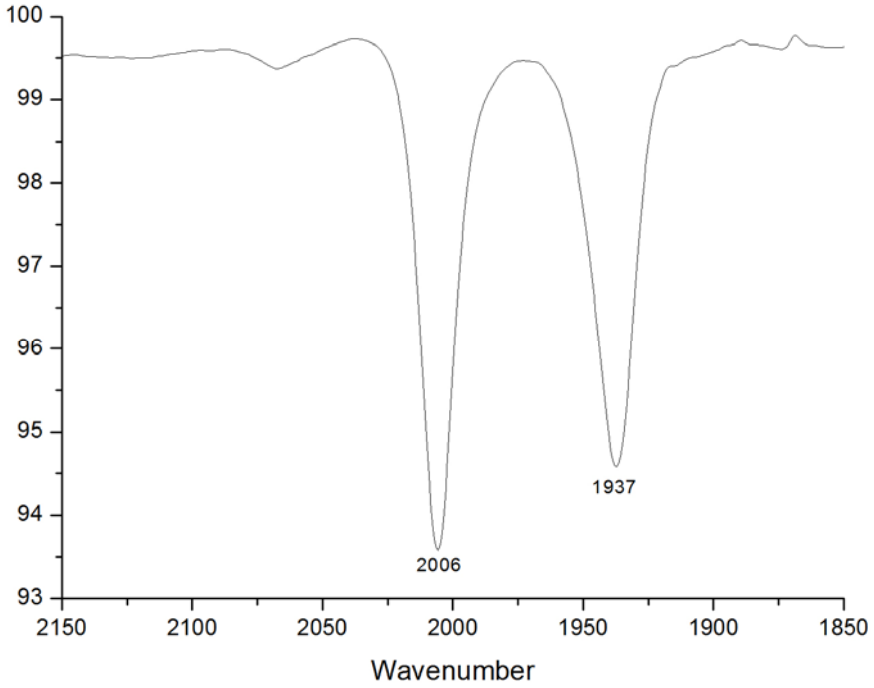

Figure S23. IR spectrum of **12** in CH_3CN.

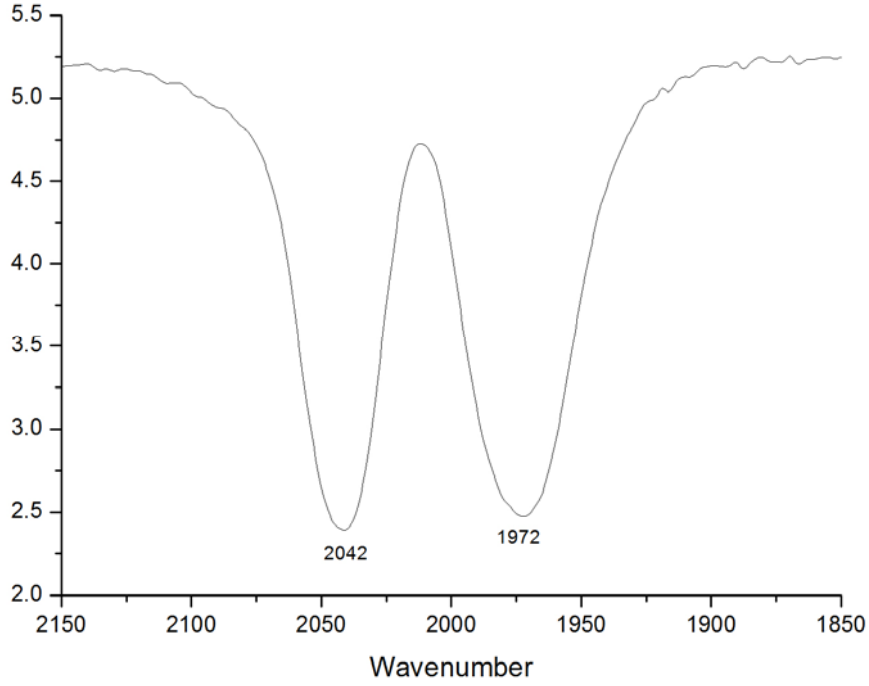

Figure S24. IR spectrum of **13** in the solid state.

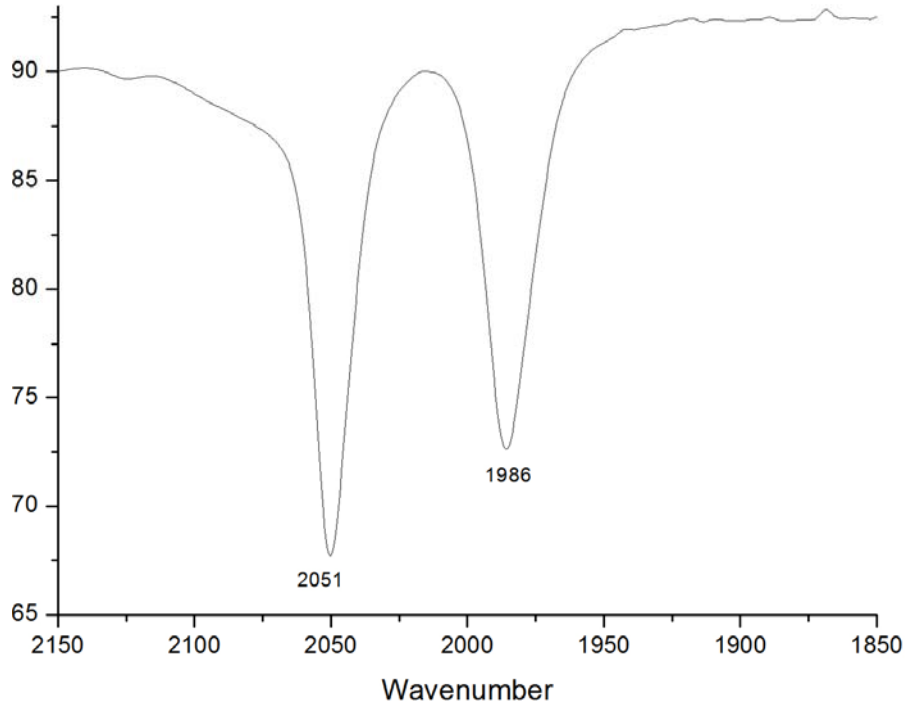

Figure S25. IR spectrum of **13** in CH_2Cl_2.

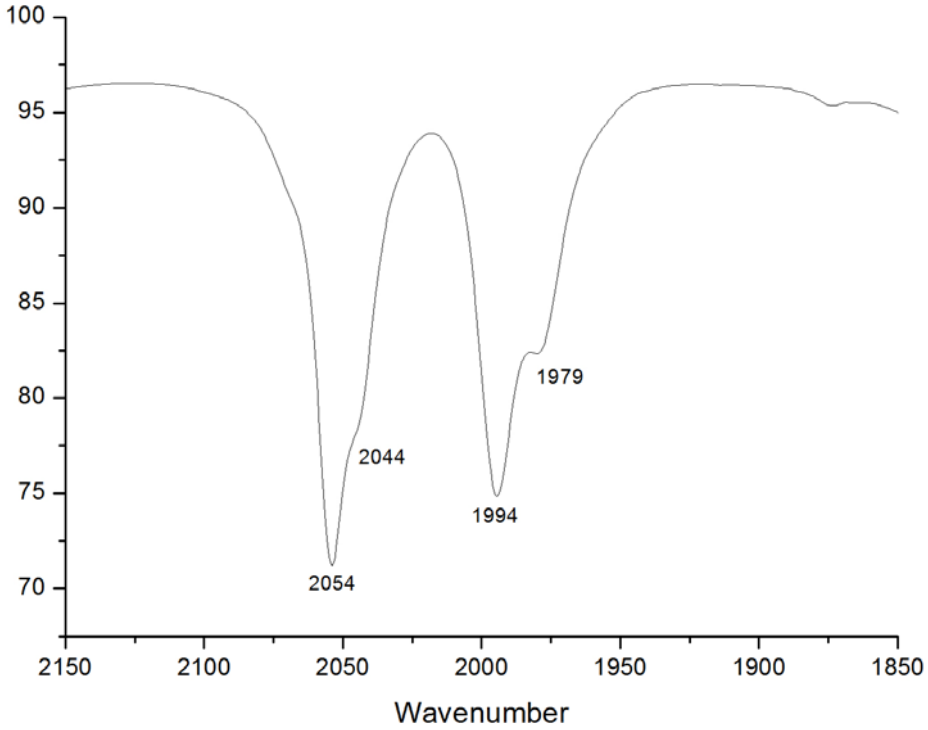

Figure S26. IR spectrum of **13** and **13a** in CH_3CN.

NMR spectra

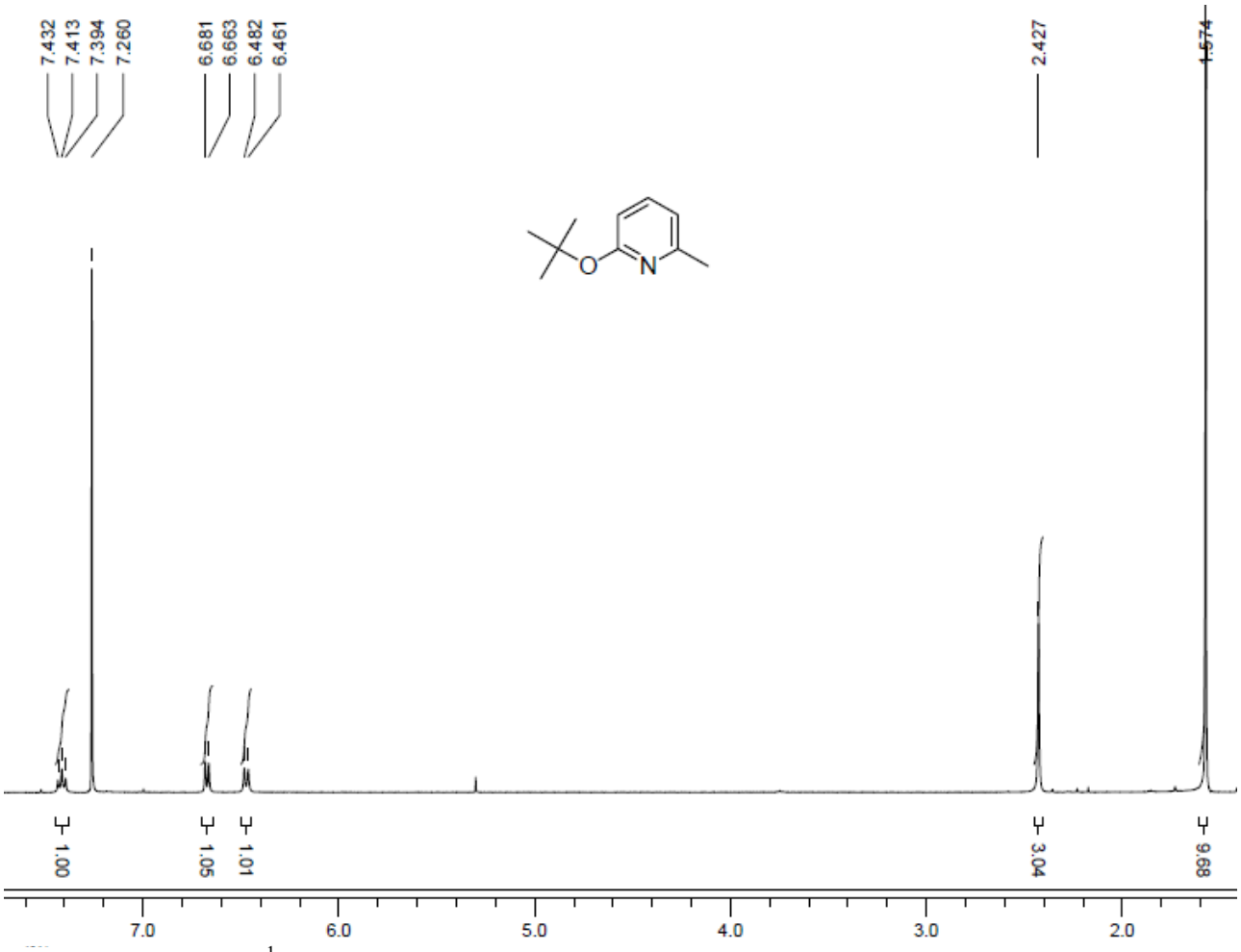

Figure S27. ^{1}H NMR spectrum of 2-*tert*-butoxy-6-methylpyridine in $CDCl_3$.

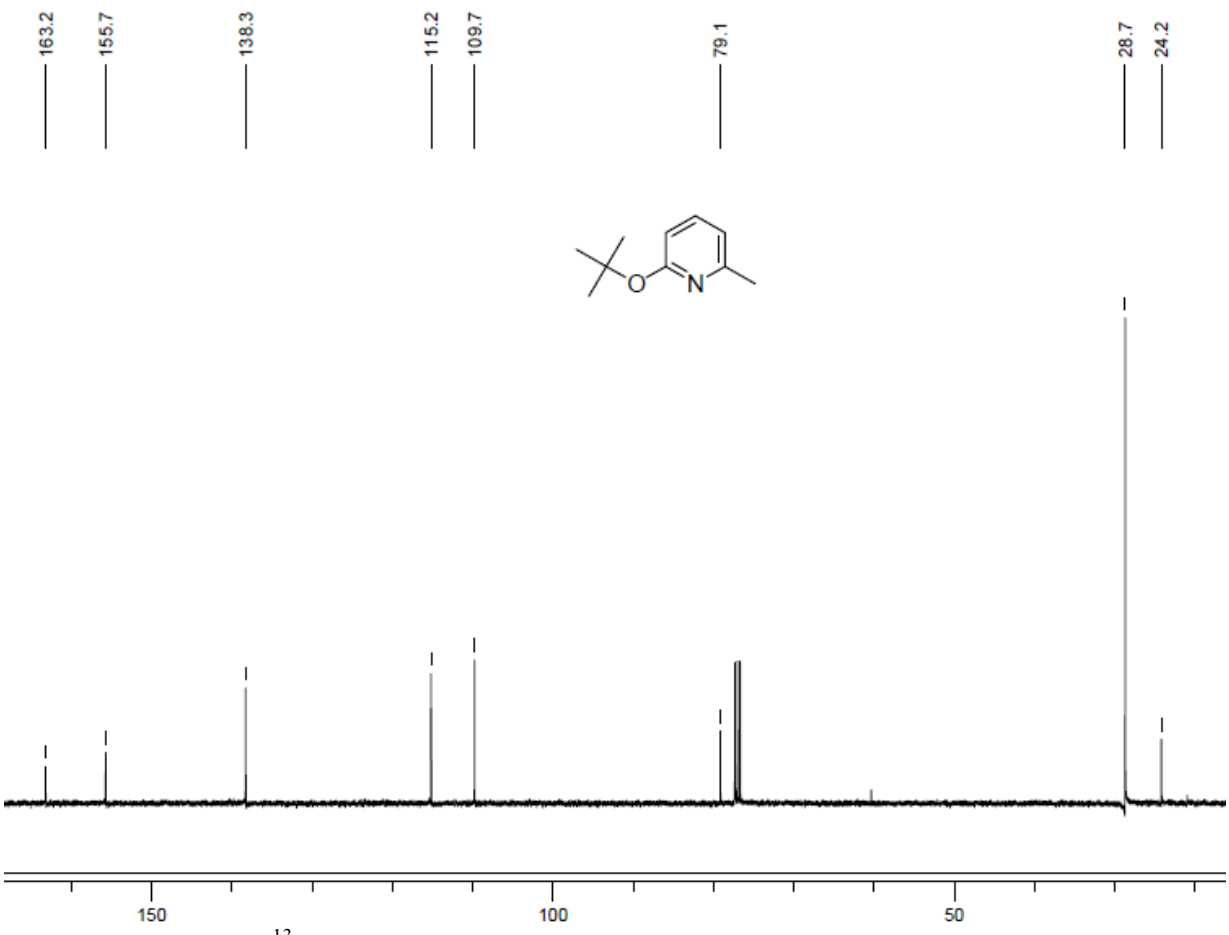

Figure S28. ^{13}C NMR spectrum of 2-*tert*-butoxy-6-methylpyridine in $CDCl_3$.

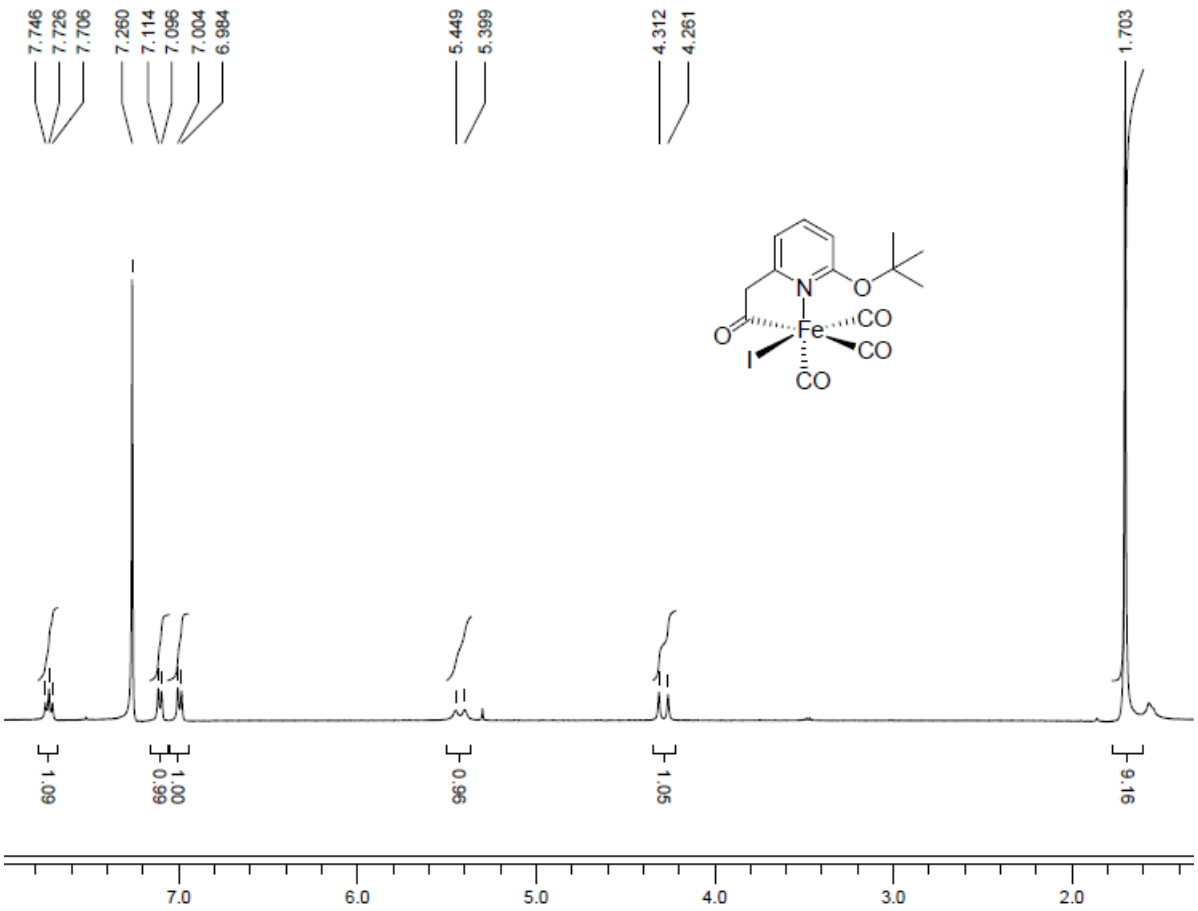

Figure S29. ^{1}H NMR spectrum of **1** in $CDCl_3$.

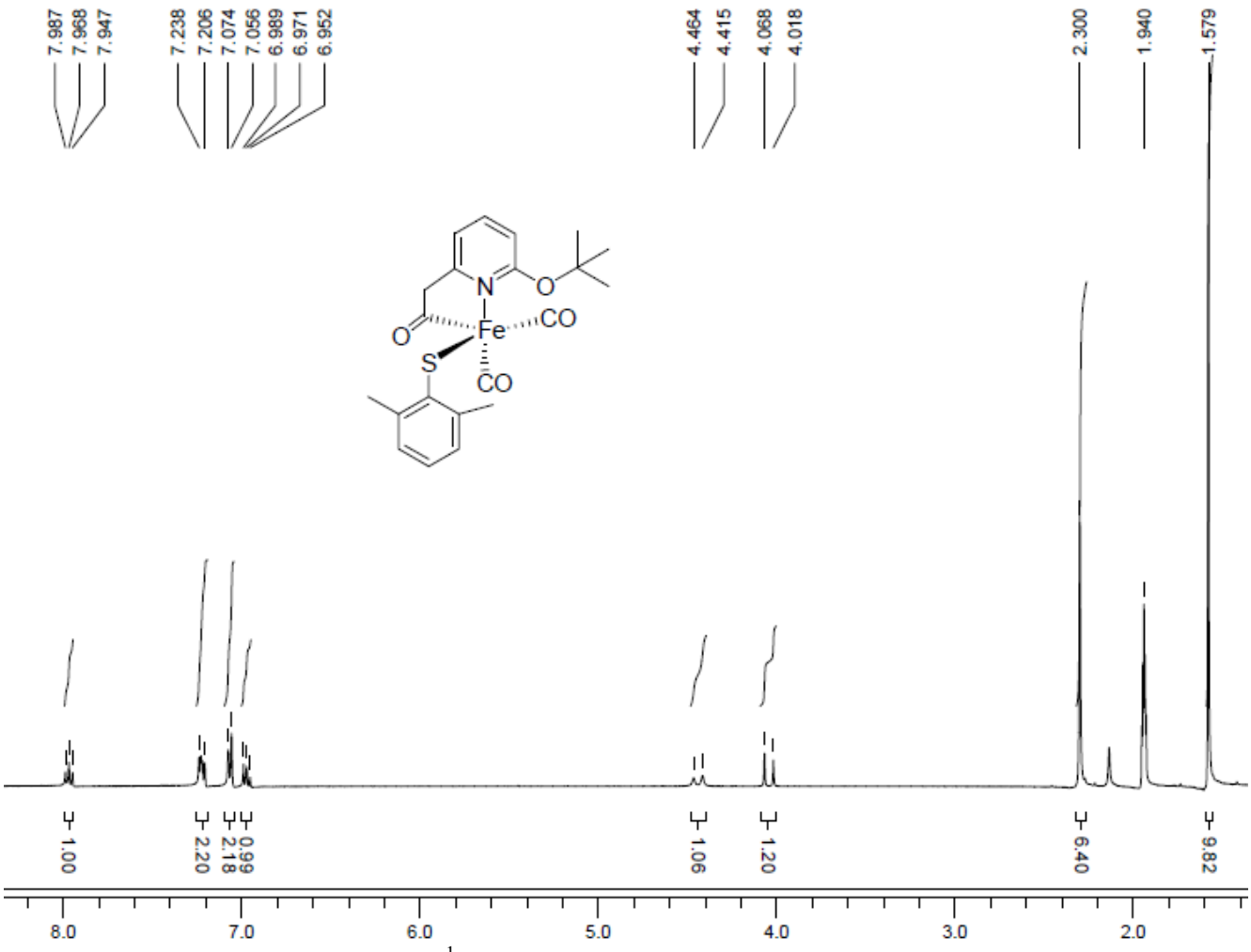

Figure S30. ^{1}H NMR spectrum of **2** in CD_3CN.

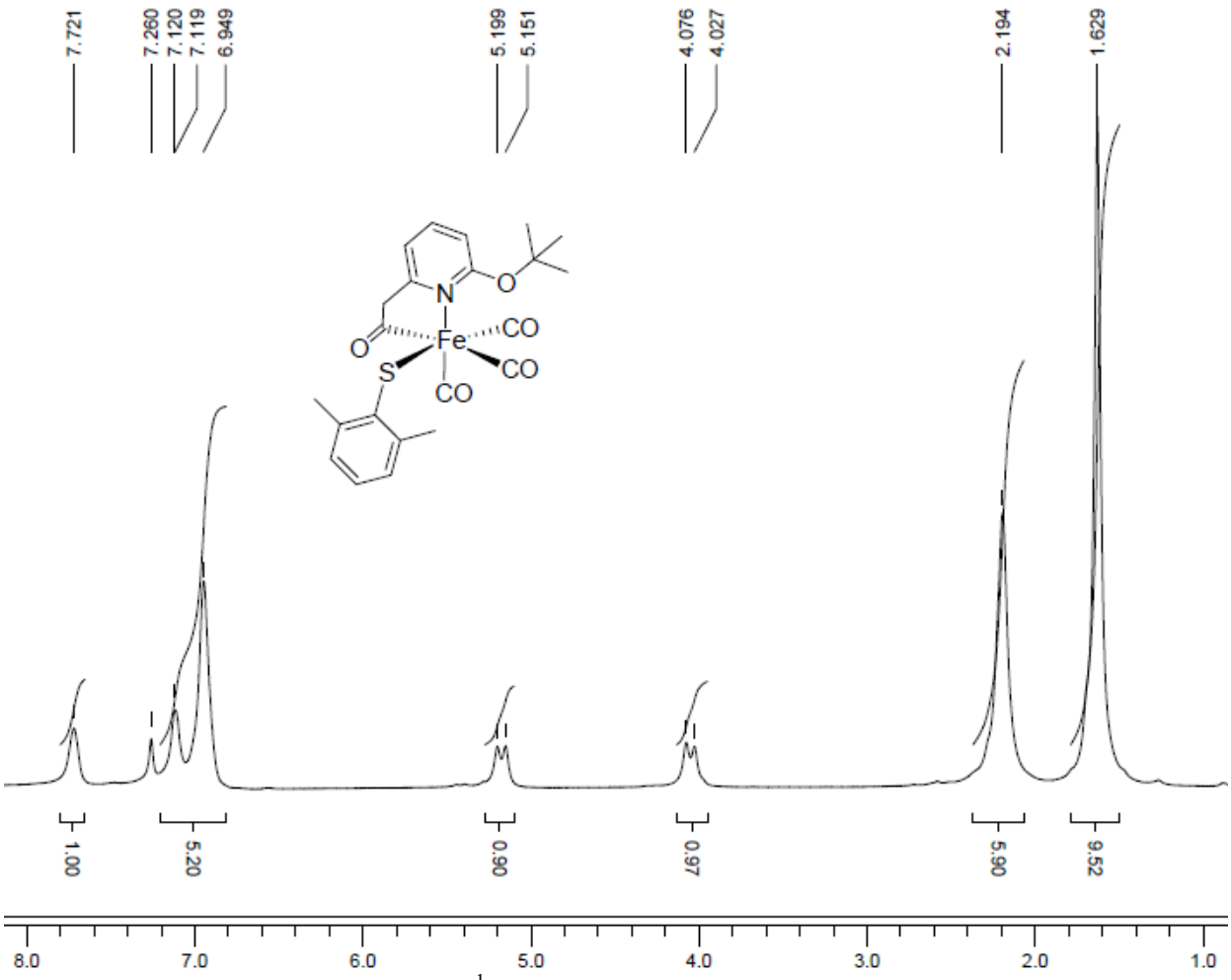

Figure S31. ^{1}H NMR spectrum of **3** in $CDCl_3$.

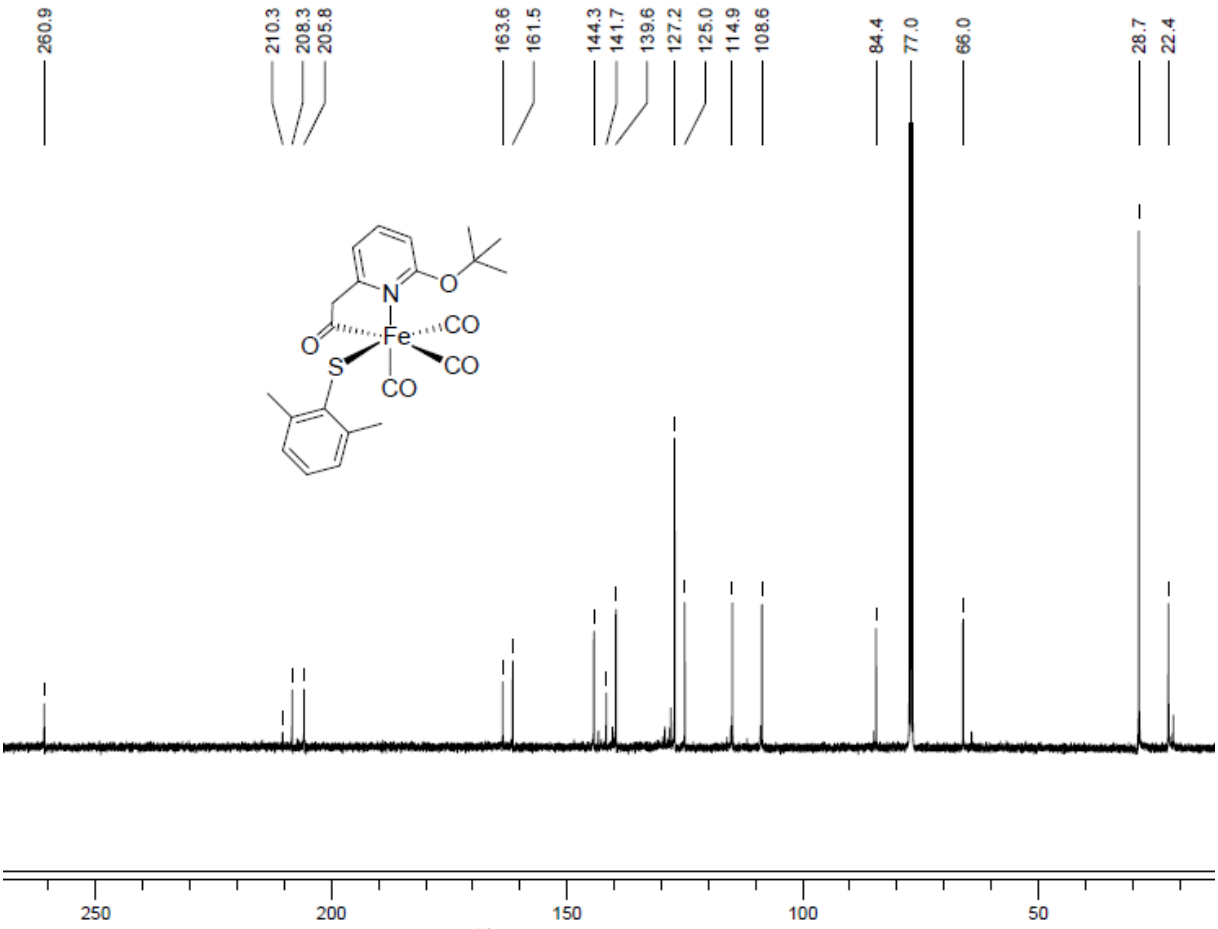

Figure S32. ^{13}C NMR spectrum of **3** in $CDCl_3$.

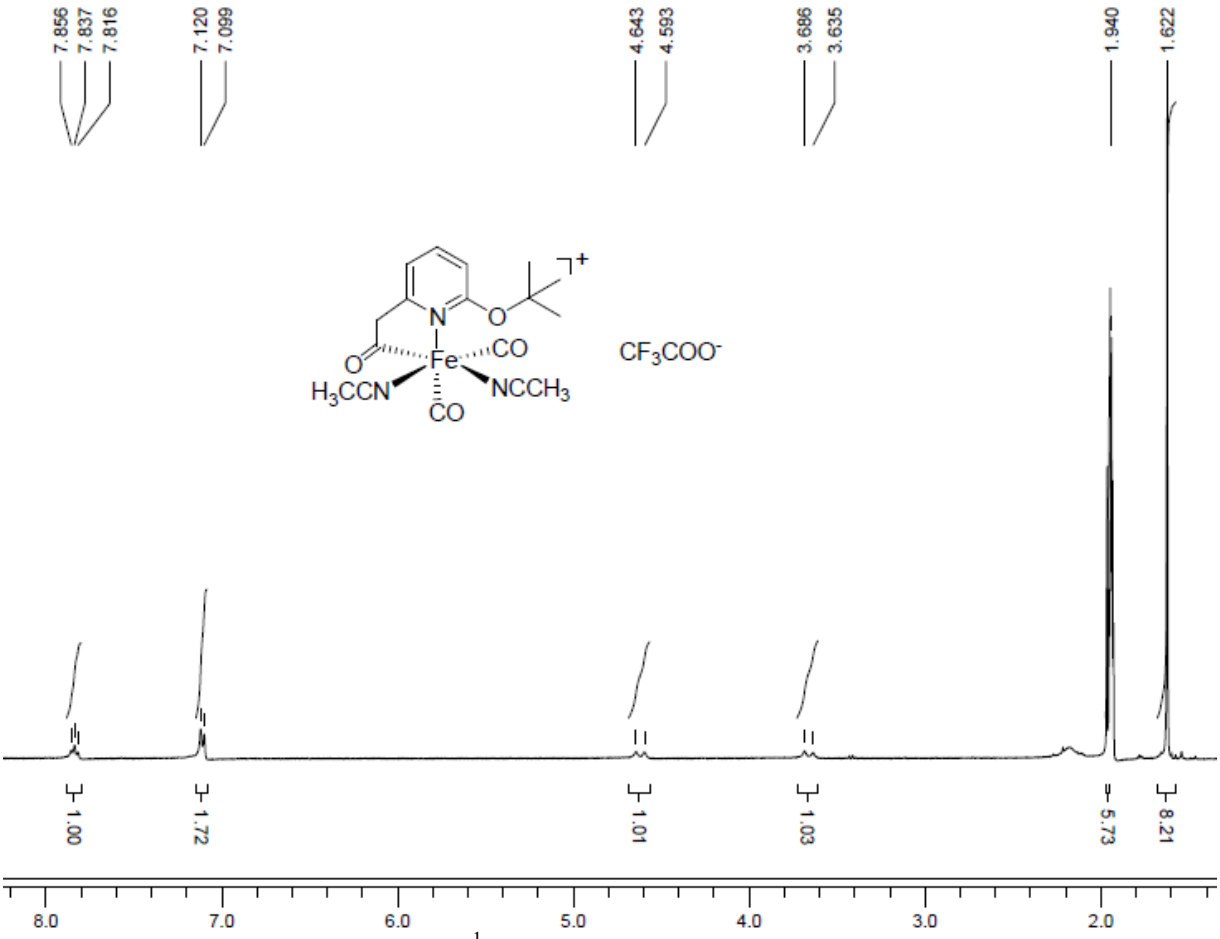

Figure S33. ^{1}H NMR spectrum of **4** in CD_3CN.

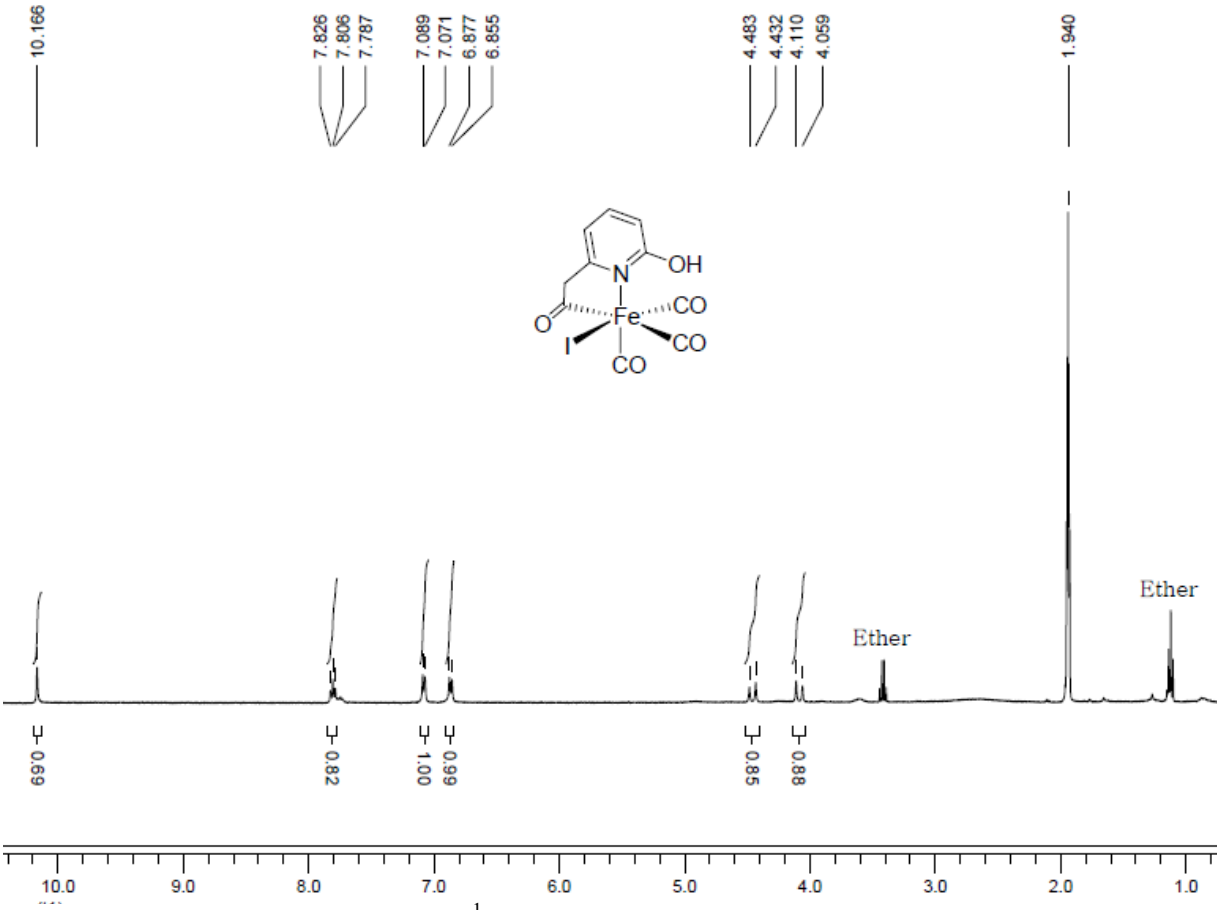

Figure S34. ^{1}H NMR spectrum of **5** in CD_3CN.

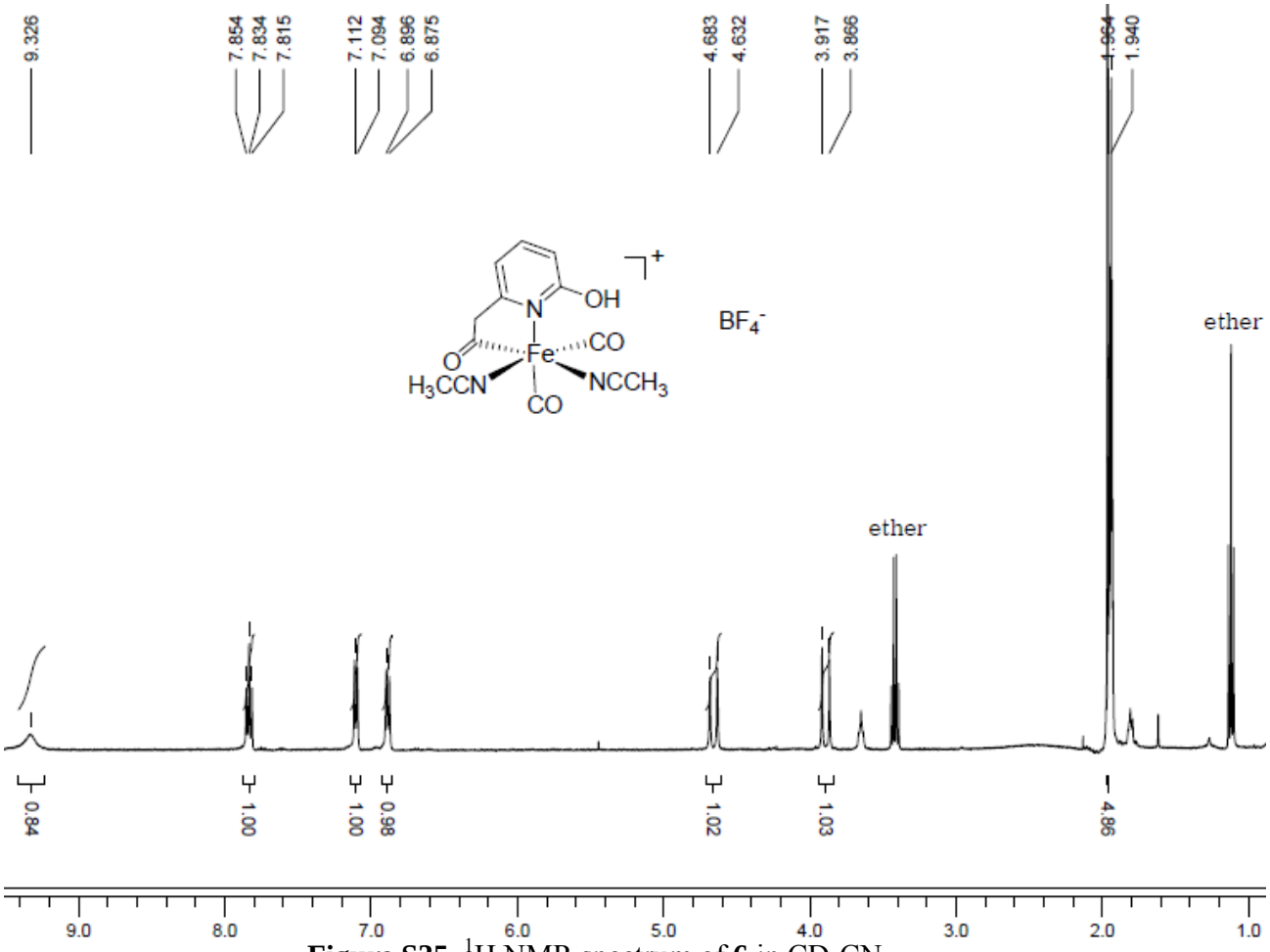

Figure S35. ^{1}H NMR spectrum of **6** in CD_3CN.

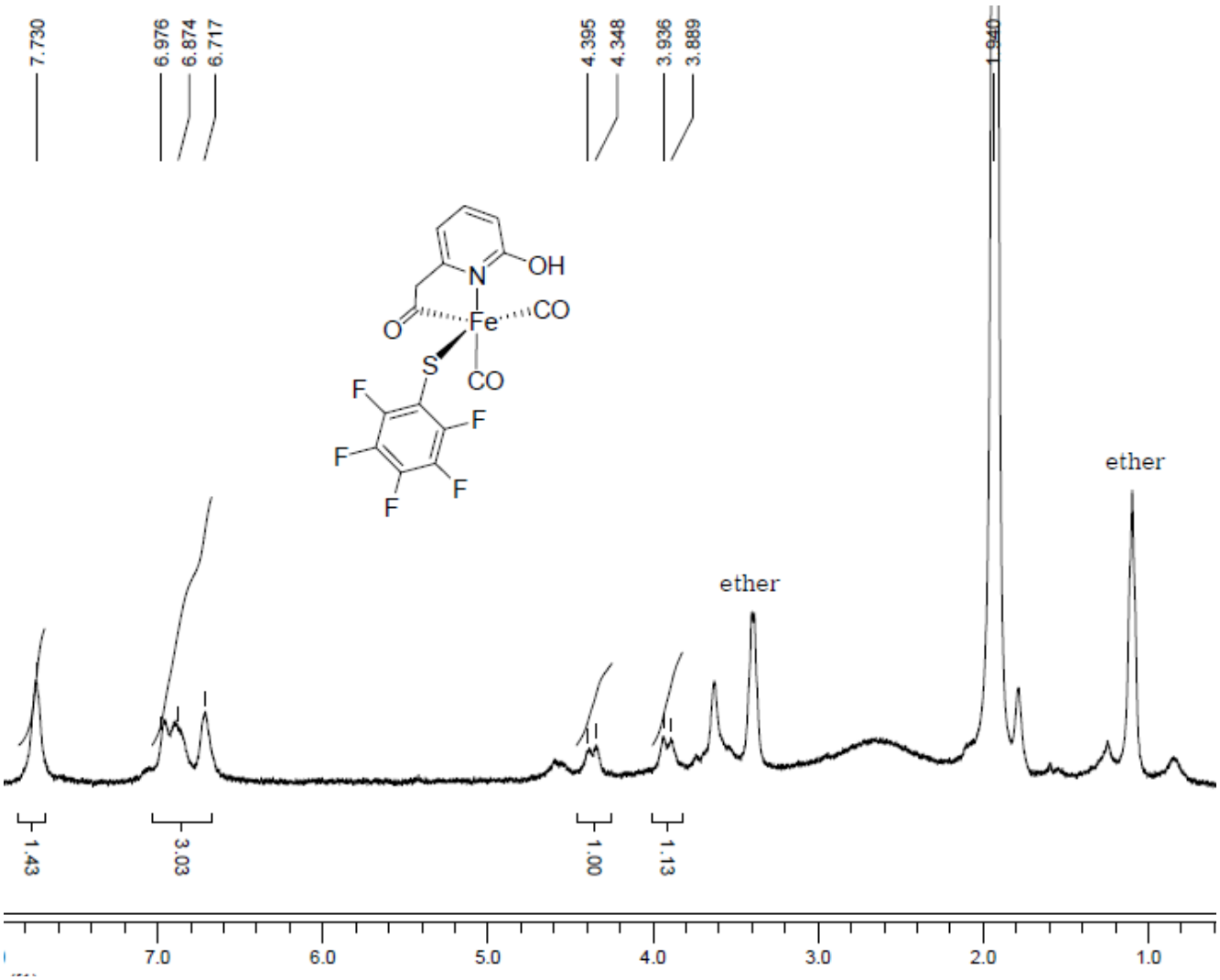

Figure S36. ^{1}H NMR spectrum of **9** in CD_3CN.

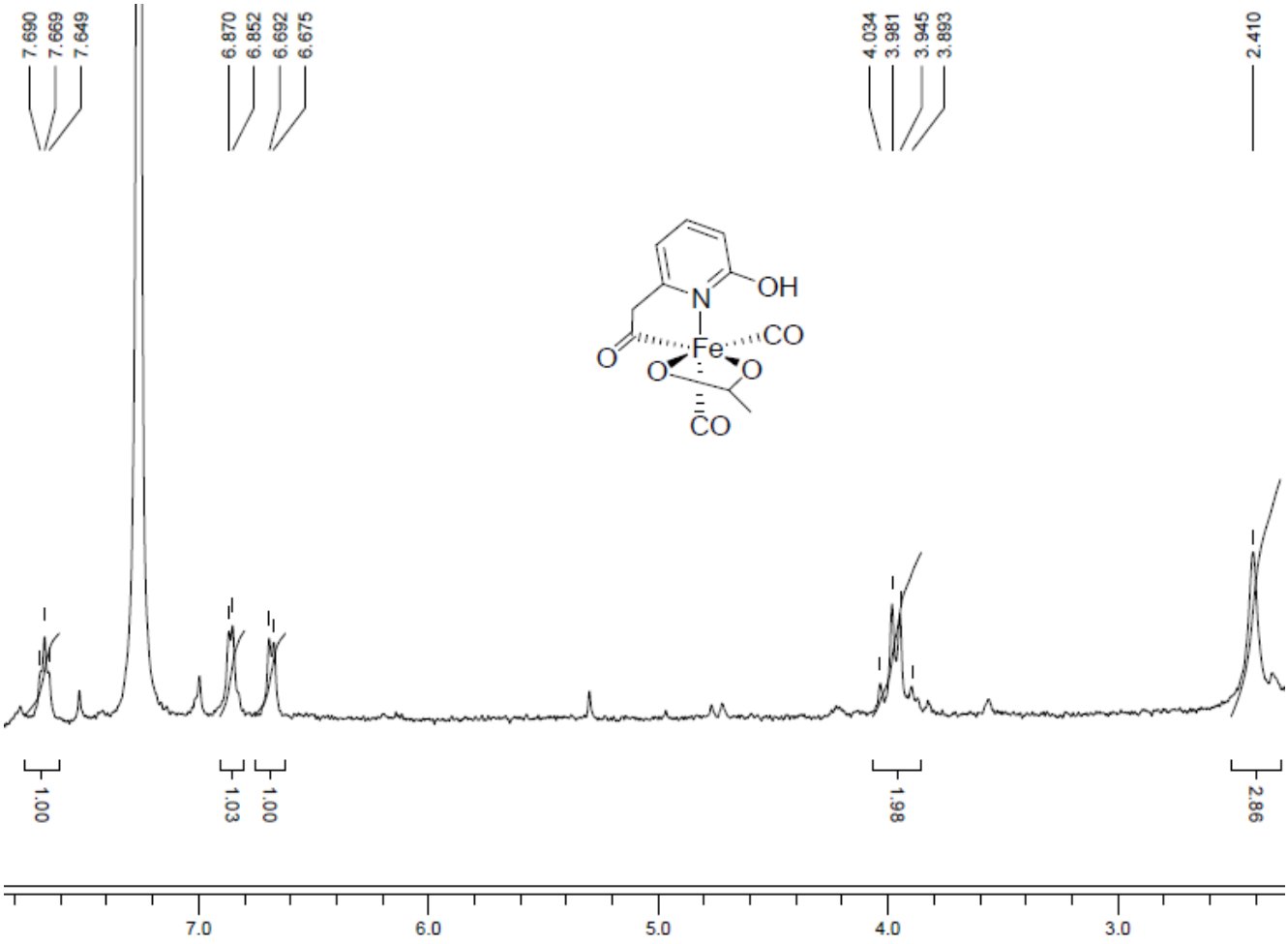

Figure S37. ^{1}H NMR spectrum of **13** in $CDCl_3$.

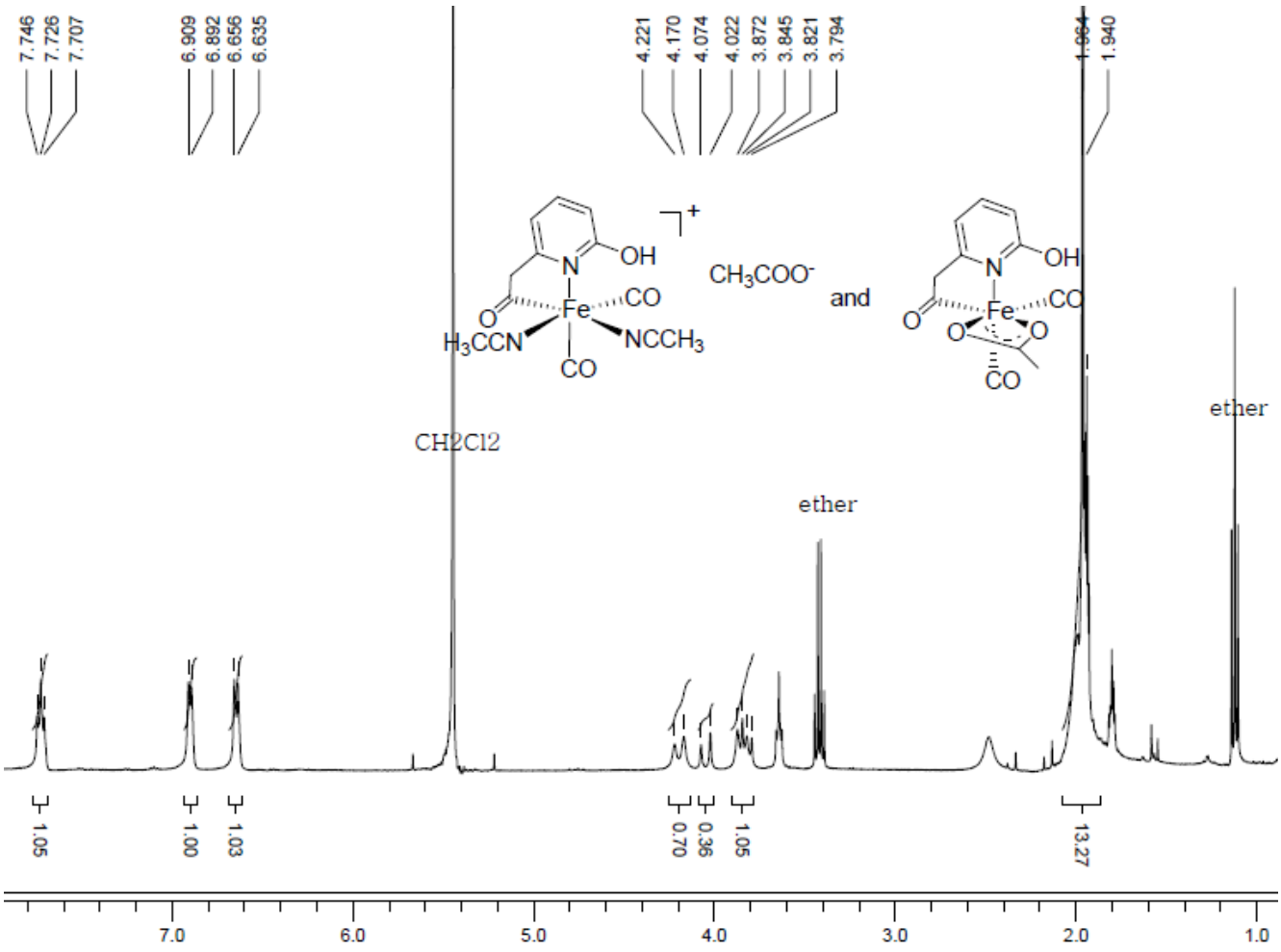

Figure S38. ^{1}H NMR spectrum of **13** and **13a** in CD_3CN.